Structure and genesis of the Boulder-Weld allochthon, Denver Basin, Colorado – Gravity slide or Laramide thrust sheet?[1]

EDWARD J. (NED) STERNE[2]

1. Manuscript received April 7, 2020; Accepted July 13, 2020

2. Independent Geologist, 1981 W. Briarwood Ave., Littleton, Colorado 80120, nedsterne@aol.com

ABSTRACT

This study was undertaken to determine the structure and genesis of the Boulder-Weld allochthon (BWA), the 216 mi^2 (559 km^2) remnant of a once larger feature, that moved east from the flank of the Front Range into the western part of the Denver Basin. This review of surface and subsurface data revealed new aspects of the BWA, especially in its western part. There, the decollement of the BWA ramps 900 feet up-section to the east from a near bedding-parallel detachment low in the upper transition member of the Pierre Shale to a bedding-parallel detachment near the base of the Fox Hills Formation. Repeated sections found in wells east of the decollement ramp demonstrate up to two miles of translation in the system. Secondary faults in the hanging wall of the allochthon include antithetic thrusts bounding pop-up structures and occasional normal faults that almost exclusively overprint the decollement ramp. The hanging wall is also cut by a postulated tear fault separating areas exhibiting different amounts of translation. The western, trailing edge of the decollement shows attenuation in its hanging wall that increases to the west. This part of the decollement either represents a very low-angle breakaway normal fault or a thrust fault cutting slightly down-section in the direction of transport. Past studies perceived a southeast transport direction for the BWA in contrast to the northeast slip directions on nearby Laramide thrusts, a difference used to interpret the allochthon as a gravity slide. However, similar east-west oriented slickenlines on thrusts across the western part of the allochthon and into the neighboring Front Range leave open the possibility the BWA originated as a Laramide thrust sheet. Furthermore, both the BWA and Laramide thrusts in the neighboring Front Range utilized detachments near the top of the Pierre Shale, suggesting a possible common genesis. Given the available data, both the gravity slide and Laramide thrust models provide viable explanations for the BWA.

INTRODUCTION

Laramide fault geometries along the eastern flank of the Colorado Front Range are complicated and have been interpreted in a wide variety of ways (Erslev, 1993; Sterne, 2006). The Laramide thrust systems consist of stacked triangle zones developed along bedding-parallel detachments that create crosscutting arrays of fore- and back thrusts (Erslev and Selvig, 1997; Sterne 2006, 2019). Between Rocky Flats (south of Boulder) and Longmont there is a system of faults covering 216 mi^2 (559 km^2), called here the Boulder-Weld allochthon (BWA), that steps 20 miles east of the Laramide thrusting along the mountain front (Fig. 1). In map view, the BWA appears to be distinct from the Laramide systems and it has been interpreted as a gravity slide (Kittleson, 1992, 2009; Selvig, 1994). However, the BWA shares a variety of characteristics with the Laramide thrusts, including similar detachment levels and slip directions, and its genesis has remained an open question in the mind of this author.

As with the Laramide systems, the fault style and genesis of the BWA have been interpreted in a variety of ways. Haun (1968) envisioned a series of steep basement faults extending northeast from the Idaho Springs-Ralston shear zone exposed in the Precambrian basement along the mountain front. At White Rocks in the western part of the system, Weimer (1973) called the faults horst and graben features, yet showed them in cross section as reverse faults steepening with depth. He thought the faults could be shallow growth faults developed above the basement fault trend proposed by Haun (1968). This idea developed further in Rahmanian (1975), Davis and Weimer (1976) and Weimer and Davis (1977) where the faults were interpreted as growth faults soling into the middle part of the Pierre Shale. Davis (1980) interpreted seismic data in the Rocky Flats area and along the mountain front to show vertical faults extending into the basement. Spencer (1986) showed a style of steep normal and reverse faults rooted at depth above the Hygiene Sandstone Member of the Pierre Shale that he attributed to Laramide deformation along the mountain front. Kittleson (1992, 2009) used oil and gas wells to convincingly show the faults in the eastern part of the BWA are decollement thrusts detached near the top of the Pierre Shale rather than deep-seated faults. He recognized a single level of bedding-parallel detachment and attributed the faults to southeast-directed gravity sliding triggered by Laramide uplift and offset of the detachment by the Longmont fault, a basement wrench fault mapped by Weimer (1996). Similarly, Selvig (1994) showed faults near Marshall as decollement thrusts detached in the upper part of the Pierre Shale. He saw these as gravity-driven, southeast-directed toe thrusts based on his analysis of kinematic fabrics. Trudgill (2015) proposed a model of listric growth faults inverted by later thrusting based on his examination of outcrops near Marshall.

This work is part of an ongoing effort by the author to understand the complicated fault geometries along the eastern flank of the Front Range. It was initially undertaken to: 1) better understand the western parts of the BWA reported by Kittleson (2009) to include a breakaway zone in the White Rocks area (Fig. 1) for his proposed gravity slide, and 2) to explore a possible link between Laramide thrusting and the BWA indicated by their shared detachment levels near the top of the Pierre Shale (Sterne, 2006) and their similar transport directions as indicated by slickenline orientations reported by Selvig (1994). The original goal was to build one cross section from the mountain front across the BWA, but the study expanded to include a full review of the BWA once it became evident the western part of the system was different than previously shown.

Geometries of the BWA will be illustrated using information from this detailed study of surface and subsurface data. The study builds on past investigations reported in the literature and combines these with mapping based on resistivity logs in over 1100 oil and gas wells and lithologic logs from hundreds of water wells. Fieldwork focused on clarifying earlier descriptions of faults and finding new fault exposures. These data provide a more complete picture of the structure of the BWA. What remains more elusive is its genesis. I will show that both gravity slide and Laramide thrust origins are viable models for the BWA. Unfortunately, the answer to this puzzle may have been removed by the erosion of structures that once lay between the Laramide mountain front and the western margin of the allochthon.

PREVIOUS INVESTIGATIONS

This study draws on a wealth of prior work. Faults related to the BWA first appeared on the maps by Emmons et al. (1896) and were incorporated into the mapping of the Boulder district by Fenneman (1905). An original, unpublished plane table map by H.A. Aurand (circa 1920's) capturing structural details of the White Rocks area resides

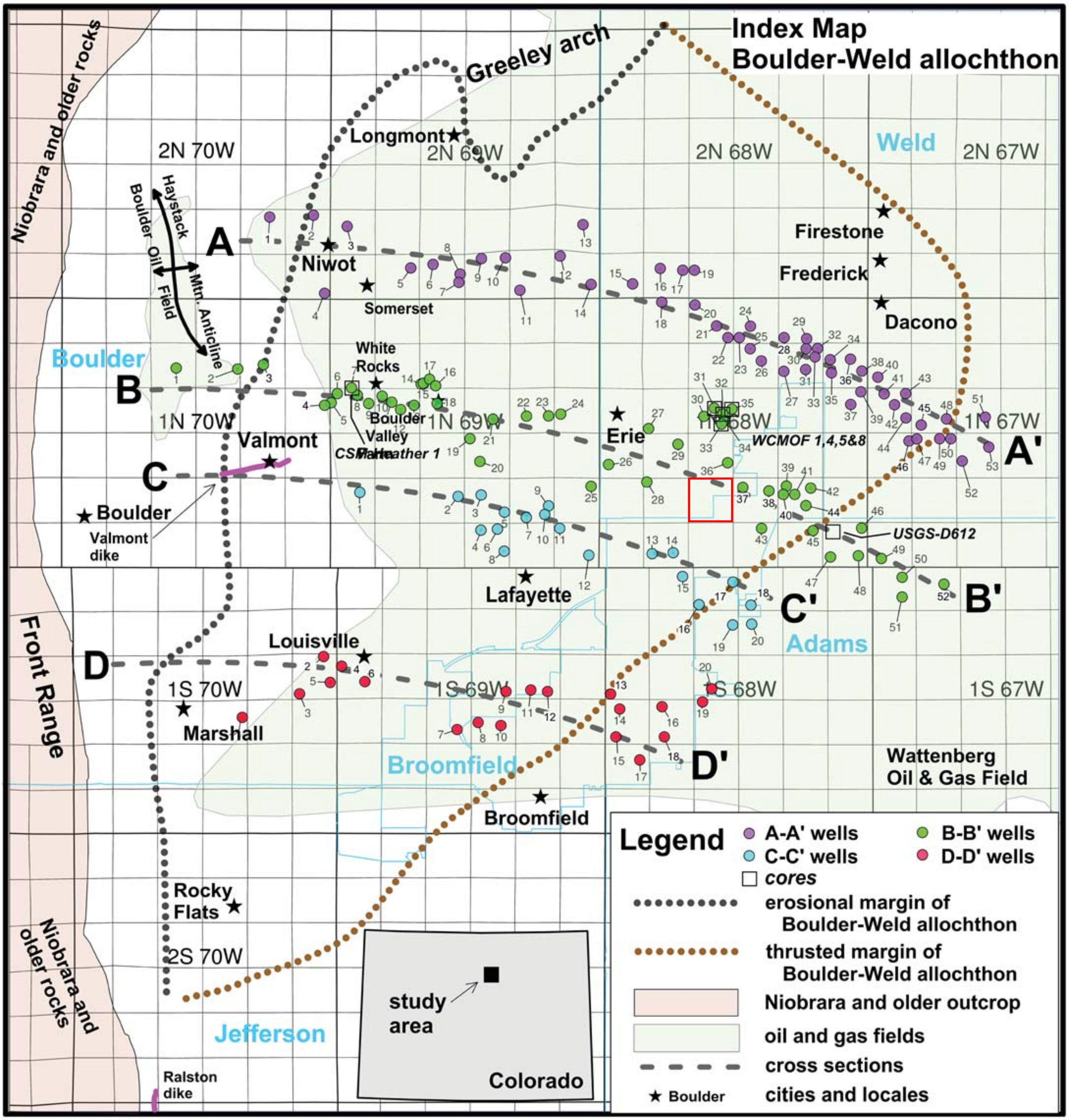

Figure 1. Index map, Boulder Weld allochthon (BWA). Figure shows the location of the BWA east of the Front Range and on top of the southwestern portion of the Wattenberg oil and gas field. Wells and cores are shown that have been incorporated into four cross sections.

in the Denver Earth Resources Library. Detailed 7.5 minute quadrangle mapping commenced with the work of Spencer (1961) in the Louisville quadrangle showing faults exposed near Marshall. Subsequent maps at this scale are available for the Boulder (Wrucke and Wilson, 1967), Eldorado Springs (Wells, 1967), Erie (Colton and Anderson, 1977), Frederick (Keller and Morgan, 2018), and Niwot (Trimble 1975) quadrangles. More regional 30 by 60 minute quadrangle maps covering the BWA include Denver West (Kellogg et al., 2008) and Estes Park (Cole and Braddock (2009). Scott and Cobban (1965) augmented the surface mapping of these areas by defining and mapping faunal zones within a thick and poorly exposed expanse of Pierre Shale along the western margin and of the BWA.

Poor bedrock exposures made mapping of faults across much of the BWA dependent on subsurface information from coal mines. Faults encountered in the mines between Erie and Firestone were mapped by Colton and Lowrie (1973). Expanding on this effort, Spencer (1986) presented a detailed structure map of the principal mining target, the Laramie Formation C Coal that lies immediately above the Fox Hills Formation. Roberts et al. (2001) expanded on Spencer's work with a more generalized map depicting the whole of the Boulder-Weld fault zone, which comprises the eastern margins of the BWA. Kittleson (1992, 2009) used oil and gas well data to characterize decollement thrust geometries across the BWA. Selvig (1994) mapped thrusts and associated kinematic fabrics in the Marshall area. More recently, Trudgill (2015) used the surface features near Marshall to illustrate the utility of digital mapping techniques. Along the southern margin of the BWA, trench profiles across faults, and shallow seismic surveys were used to assess possible earthquake hazards at the Rocky Flats nuclear bomb trigger plant (Davis, 1980); Ebasco Team (1992, 1993a). Seismic data designed to image deep structure have been presented for Rocky Flats by the Ebasco Team (1993b) and a pre-stack depth migration of this line has been incorporated into a palinspastic restoration of the mountain front west of Rocky Flats by Sterne (2019).

METHODS AND DATA

OIL AND GAS WELLS

For this study, structure of the BWA was mapped using subsurface information from over 1100 resistivity logs run in vertical oil and gas wells and available on the Colorado Oil and Gas Commission (COGCC) website. Well data not available through the COGCC were obtained from the Denver Earth Resources Library. Well logs for many of these wells end at or below the BWA decollement and only provide direct or projected control for its structure. A smaller subset of wells has logs extending up into the hanging wall of the decollement, and yet a smaller subset crosses secondary faults branching off the decollement. Where shallow data were available, sixteen marker horizons were picked starting with the K-0 horizon at the top of the Baculites *clinolobatus* zone, equal to the base of the upper transition member of the Pierre Shale, and ascending to the K-15 horizon in the upper part of the Fox Hills Formation (Fig.2). These markers represent approximate timelines and are recognizable across the study area. In addition, the Fox Hills Formation top was carried as a useful facies boundary rather than as a strict time horizon as the 17th and highest of the well log picks. It must be emphasized that facies types, characterized by shales of the Pierre Shale, sandstones of the Fox Hills Formation, and coals with mixed shales and sandstones of the Laramie Formation, do not follow timelines; rather they climb across the time horizons from west to east as part of the prograding shoreline of the retreating Cretaceous Seaway (Dechesne et al., 2011). Therefore, a timeline might be bounded by Laramie coal facies on the west, by Fox Hills sandstone facies farther east, and Pierre shale facies even farther east. The structural detachments parallel the marker horizons rather than facies boundaries, which is important to understand when comparing structure in different parts of the BWA. Note for example, the base of the Fox Hills sandstone facies lies approximately 300 feet deeper in the section in the western part of the study area than where encountered 15 miles to the east (Fig. 2).

Tracking numerous stratigraphic horizons through the large number of wells penetrating the BWA is what allows the details of the structure to be revealed. The lowest of these, the K-0 horizon is a marker in the regional section just below the decollement in the western part of the BWA. It was mapped to understand the structure of the regional layer in relation to the overlying decollement and to determine if the decollement ramped through it at any point. The decollement is at the K-1 horizon along the western part of the BWA and climbs to the K-5 horizon to the east (Fig 2). Picking numerous horizons below, at, and

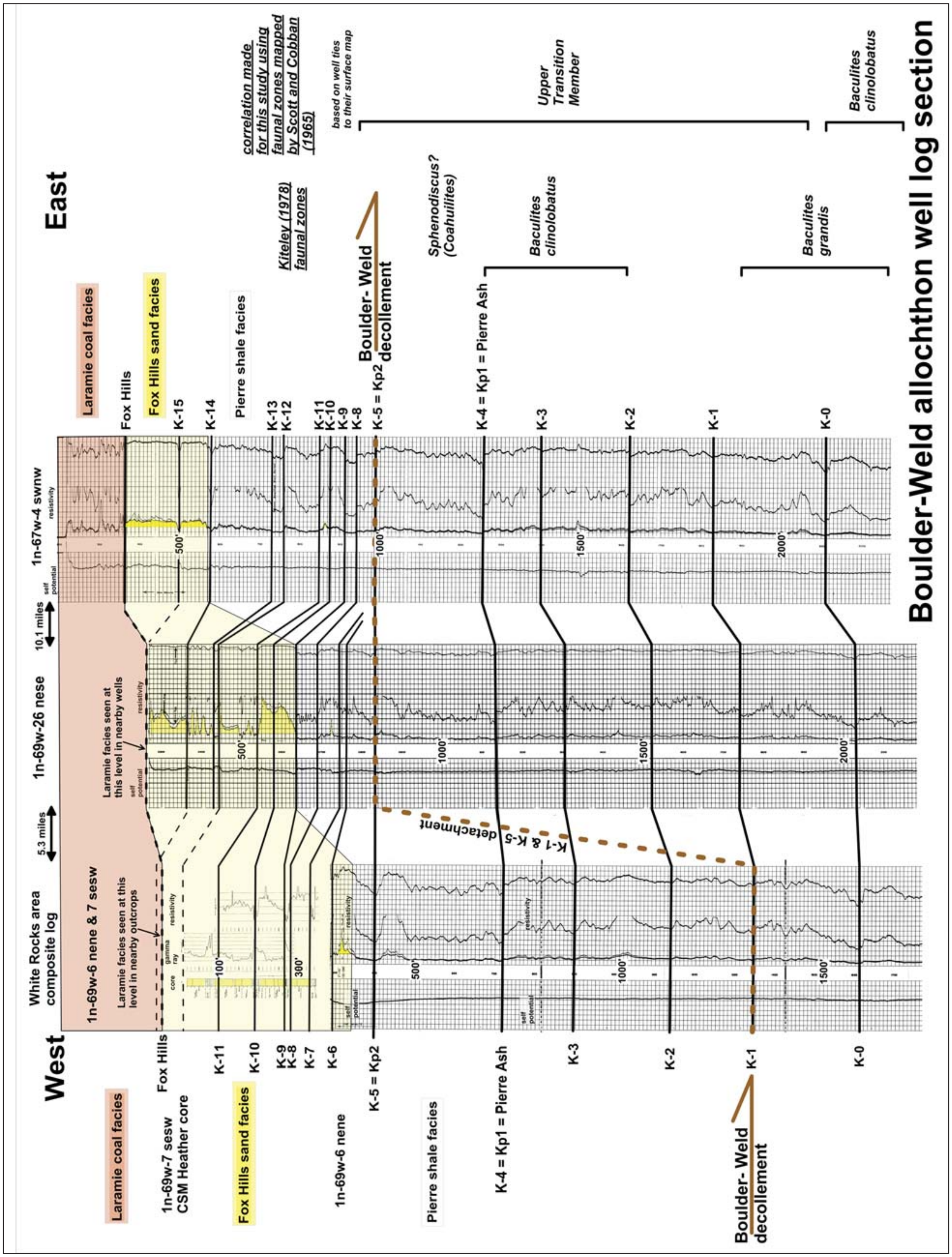

Figure 2. Well log transect of the Boulder-Weld allochthon (BWA). Figure is a log cross section that spans the BWA. It shows the horizons picked in over 1100 wells for this study. Note how facies tracts climb section to the east. The BWA decollement ramps eastward from the K-1 horizon to the K-5 horizon of the upper transition member of the Pierre Shale.

above the decollement made it easier to track and characterize faults in its hanging wall. Deep picks were also made down to and including the top of the lower Cretaceous J Sand-Muddy Formation of the Dakota Group to better understand any structures in the regional layer that might impact the BWA.

WATER WELLS AND SPENCER'S (1986) COAL MINE STUDY

Hundreds of water well lithologic logs available on the Colorado Division of Water Resources website were examined across the western part of the BWA to determine near-surface patterns related to deeper structure. Because of poor surface exposures, these logs were often the only data available in the absence of shallow oil and gas well data. They typically contained enough information to identify the three principal facies of the shallow section: 1) shales of the Pierre Shale, 2) sandstones of the Fox Hills Formation, and 3) mixed coal, shale and sandstones of the Laramie Formation. Water wells were only studied in areas beyond Spencer's (1986) shallow structural study of the eastern part of the BWA, which was based on coal mine maps, coal exploration cores, oil and gas wells and water wells.

CORES

This study included examination of the Heather #1 core (SE SE SW 7, T1N, R69W, Fig. 1) obtained by the Colorado School of Mines and available in its core laboratory. This core is described in detail in Weimer and Tillman (1980). Geophysical logs of the core are included in Bedwell (1974) and Davis and Weimer (1976). Weimer and Tillman (1980) also measured sections of the Fox Hills Formation exposed on either side of the Big fault at White Rocks immediately south of the Heather core location. The outcrop data, shallow data from the Heather core and nearby water wells were integrated with deep information from oil and gas wells to understand structure across the White Rocks area (Sterne and Raynolds, 2019).

The lower part of USGS core number D612, located just east of the mapped margin of the BWA (NW NW 36, T1S, R68W, Fig. 1), was examined at the USGS Core Research Center. This core offers a complete reference data set for the upper part of the Pierre Shale, the Fox Hills Formation, and the Laramie Formation. The bentonitic K-4 horizon appears at ~1120' (Kp1 marker of Kittleson (1992, 2009); Pierre Ash of Dechesne et al. (2011)). At ~1076', the estimated level of the K-5 detachment (Kp2 marker of Kittleson (1992, 2009)), there is an interval of finely brecciated shale, a texture not seen elsewhere in the part of the core we examined (1065'-1487'). This point deserves further study, because the brecciated shale could relate to slip along the K-5 detachment, suggesting the BWA extends farther southeast than currently mapped.

Data from four cores cut for the site planning of the Weld County Meteorological Observing Facility (16, 1N, 68W) were provided by CTL Thompson, Inc. and a copy of the report has been given to the Colorado School of Mines core laboratory. The report by Ameudo and Ivey (1975) includes detailed core descriptions and geophysical logs. The facility was located on an upthrown thrust block between areas mined for coal and the cores provide a unique set of data across the shallow bounding faults (Fig. 1).

FIELDWORK

Fieldwork for this study focused on structure and stratigraphy of the White Rocks area in the western part of the BWA (Plate 4) (Sterne and Raynolds, 2019), but included field checks of outcrops and mapped fault trends across all of the BWA.

MAPS AND CROSS SECTIONS

Well tops were picked and structure maps were contoured using Petra™ software. The maps were prepared using a geographic projection and a Nad27 datum. Cross sections were made using LithoTect™ software, a program that facilitates cross section construction and palinspatic restoration. Surfer™ software was used to draft some of the maps and to annotate the maps and cross sections created in the other programs.

Four cross sections were drawn to follow the arc of a postulated tear fault, as discussed below, that divides areas showing different amounts of translation. The sections were originally drawn with an east-west orientation paralleling the transport direction indicated by slickenline orientations across the western part of the BWA. However, this alignment was abandoned once it became apparent that a section drawn across the central portion of the BWA showed significantly greater translation to the east than to the west. This would only make sense if normal faults were developed between the western and eastern parts of the system, for which there is no evidence. Once the postulated tear fault was recognized, sections drawn on either side of it showed translation consistently decreasing to the east in a manner compatible with the observed structures. The cross sections extend west to basement outcrops along the eastern margin of the Front Range. Details of the Laramide thrust geometries along the mountain front have been addressed by the author (Sterne, 2006, 2019) and a restorable cross section showing Laramide thrust geometries across the mountain front at the latitude of the Haystack Mountain anticline is presented below.

Plates 1 and 2 show the upper part of the cross sections above the K-0 horizon, which is the shallowest horizon mapped in the regional layer. The regional layer refers to rocks below the allochthon. These detailed sections are shown with no vertical exaggeration and include nodes on the wellbores corresponding to horizon picks. The tops and bottoms of logged intervals are marked by black circles with white centers. Well nodes and horizons shown above and below the limits of the available logs are projected. Wells were projected typically a mile or less into the sections (Fig. 1). Wells with data restricted to the footwall of the allochthon or that showed no faulting above the decollement were projected into the line of section parallel to the local strike of the regional layer. Wells showing faulting above the decollement were projected into the line of section parallel to the trend of local hanging wall structure shown on the maps of Spencer (1961, 1986) and Roberts et al. (2001). This approach typically worked well, but because the decollement tracks regional layer structure (except at the ramp), projections made parallel to hanging wall structures can impart artificial structure to the decollement and the regional layer. The solution to this problem would involve projecting the hanging wall and footwall portions of the wells separately into the line of section or projecting wells down-plunge, steps not taken here. One well that deserves special mention is #3 on section A-A' (Pl. 1). It was projected into the line of section parallel to regional strike. What is not shown is that it crosses the normal fault seen also in well #4 immediately to the east. Getting both wells to accurately portray the normal fault would have involved projecting well #3 down-plunge or projecting the hanging wall and footwall portions of the well separately, again a step not taken here.

Plate 3 shows the cross sections with a vertical exaggeration of three to allow the complete sections, including the section down to the J Sand-Muddy Formation of the Dakota Group, to be shown. The sections have been extended west to show the BWA in relation to the margin of the Front Range basement uplift. To the east, the regional layer has been highlighted in green, with the elements of the allochthon highlighted in grey for the Pierre shale facies of the K-1 to K-5 interval, in yellow for the Fox Hills sandstone facies and their distal equivalents (K-6 to Fox Hills Formation top), and in brown for the mixed coal, sandstone and shale facies of the Laramie Formation.

All structures shown on the sections have been drawn so they would balance with minor adjustments in a palinspastic restoration.

RESULTS

THE REGIONAL LAYER

Understanding the structure of the BWA requires an understanding of the underlying regional layer. For this reason, structure was mapped at the K-0 horizon, which lies approximately 275 feet below the K-1 horizon, the stratigraphically lowest detachment level of the BWA decollement (Figs. 2 and 3). Regional layer structure at the K-0 horizon dips east at variable rates off the flank of the Front Range and the Greeley arch, then flattens to an approximate one degree southeast dip as it drops toward the axis of the Denver Basin. Based on outcrop dips and closely spaced well control, the K-0 horizon is folded, but not cut by discernable faults. The flexure tracking the eastern flank of the Haystack anticline and Greeley arch reflects uplift along the deep-seated Longmont fault of Weimer (1996), but the fault does not cut the K-0 horizon. This is best seen in township 2N, 69W where closely-spaced wells define an east-dipping panel above the Longmont fault. The difference in elevation between points at the top and bottom of the panel reflects eastward dip rather than offset across a fault. Wells located along the western outcrop trace of the K-0 horizon show it correlates to the top of the Baculites *clinolobatus* faunal zone, which is the base of the upper transition member of the Pierre Shale as mapped by Scott and Cobban (1965). This means the overlying BWA is developed within and above the upper transition member of the Pierre Shale.

STRUCTURE OF THE BWA DECOLLEMENT

The BWA decollement dips east off the margin of the Front Range, enters a low along the western margin of

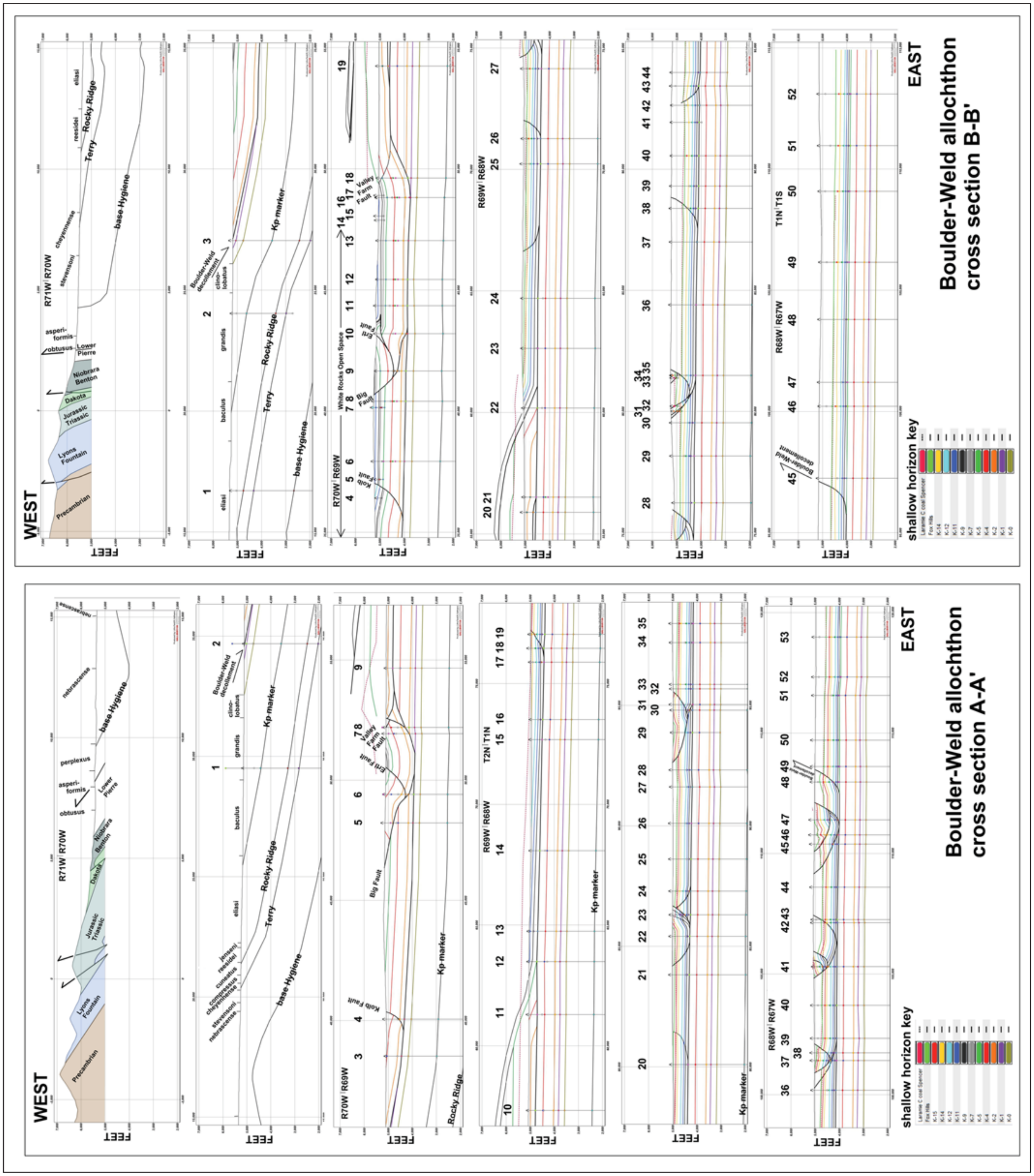

Plate 1. Detailed cross sections A-A′ and B-B′ across the Boulder-Weld allochthon.

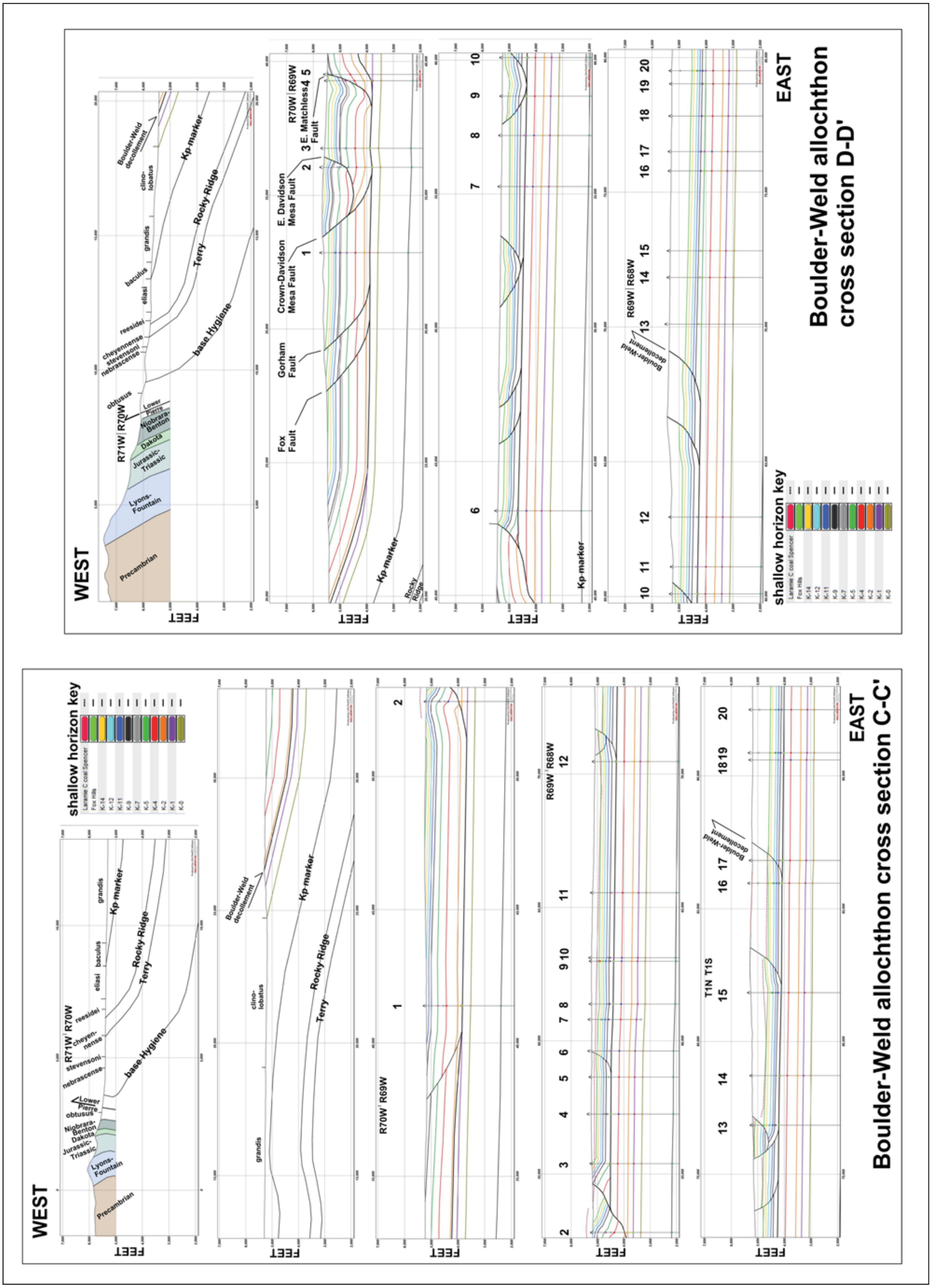

Plate 2. Detailed cross sections C-C' and D-D' across the Boulder-Weld allochthon.

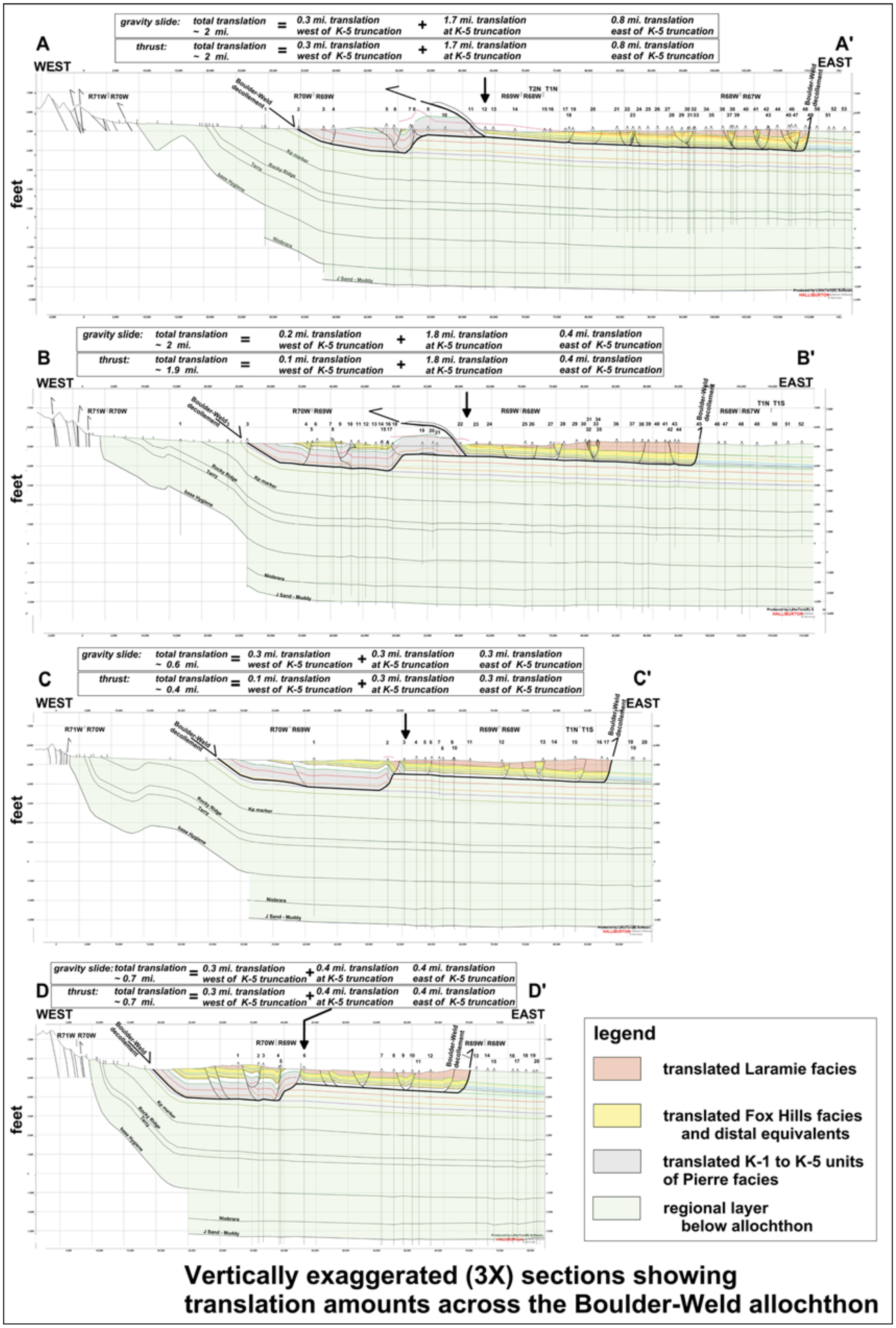

Plate 3. Vertically exaggerated (3X) cross sections showing translation amounts across the Boulder-Weld allochthon.

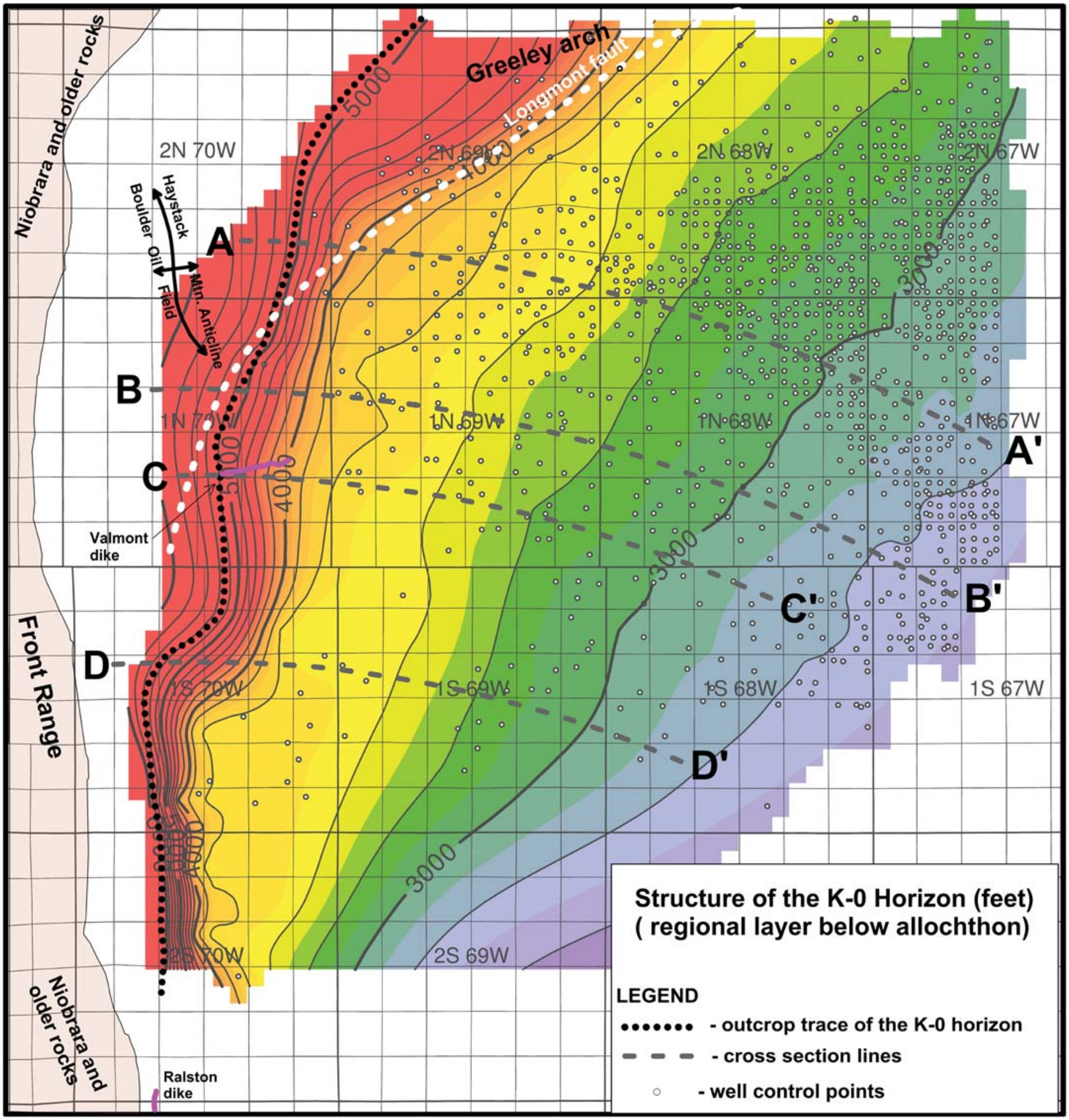

Figure 3. Structure of the K-0 horizon (feet). This map shows the regional layer below the Boulder-Weld allochthon dipping at variable rates off the flank of the Front Range and Greeley arch then dropping at a low angle toward the axis of the Denver Basin. The deep-seated Longmont fault folds but does not cut the regional layer at this level.

the allochthon, rises to the east along a thrust ramp, then follows regional dip down to the southeast to its terminus (Fig 4). The decollement closely parallels bedding at the K-1 horizon across the western part of the allochthon. East of the ramp, units between the K-1 and K-5 horizons are thrust over the shallower K-5 level of the decollement where they form a ramp anticline. East of the leading-edge truncation of the K-1 to K-5 units, the decollement parallels the K-5 horizon.

Because the decollement parallels or closely parallels bedding, except across the decollement ramp and the anticline east of the ramp, not all wells exhibit evidence of thrusting. For this reason, the level of the decollement is determined by tracking the lowest stratigraphic level of faulting in its hanging wall and by mapping horizons in its immediate footwall that show no faulting. Keep in mind that many wells lack the shallow logs needed to reveal faults above the decollement. Therefore, wells on Figure 4 that lack symbols indicating faults, either don't encounter faults above the decollement or lack the data that would show the faults.

Well control and dips of surface beds show the K-0 horizon of the regional layer and the overlying BWA decollement rise unbroken to their western outcrop traces. The decollement simply rises to the west and breaches to the surface. This means the western and northwestern margins of the BWA are erosional rather than cut by faults in the regional layer. Therefore, the current 216 mi^2 (559 km2) extent of the allochthon represents the remnant of what was a larger system. The northeastern and southeastern margins mark the currently recognized thrust limits of the BWA (Spencer, 1986; Kittleson, 1992, 2009). Wells examined several miles beyond the recognized eastern limits of the BWA show no thrusting and corroborate the allochthon margin as mapped by earlier workers.

The map also shows the northwestern limit of oil and gas well data available above the decollement. Beyond this line and extending to its outcrop trace, the decollement structure was mapped using projections from deeper horizons. In this area, surface geology and water wells provide the only information for structure above the decollement.

Deep wells west of the proposed BWA erosional trace preclude the decollement ramping down-section and rooting in the subsurface to the west. The wells give no indication of the magnitude of thrust repeat that would be required to explain the up to two miles of eastward translation shown by the BWA. In addition, the author has examined proprietary seismic data across the western margin of the BWA that corroborate the lack of an east-directed thrust in this position.

THE THRUST RAMP IN THE BWA DECOLLEMENT CONNECTING THE K-1 AND K-5 DETACHMENTS

Just east of the White Rocks and Marshall areas, the BWA decollement ramps up-section some 900 feet from a near bedding-parallel detachment at the K-1 horizon to a bedding-parallel detachment at the K-5 horizon (Fig. 2). The thrust ramp is penetrated by several wells as shown in map view and on all of the cross sections (purple dotted line on Fig. 4, Plates 1-3). The ramp and areas to the west are characterized by thrust repeats and stretched section indicating high dips in rocks down to the K-1 horizon (red diamonds on Fig. 4). East of the ramp, all faulting occurs above the K-5 horizon.

The most compelling evidence for eastward translation of the BWA and the ramp in its decollement are wells showing units between the K-1 and K-5 horizons carried east of the ramp and onto the K-5 level detachment (blue triangles on Fig. 4). Figure 5 shows the log character of the footwall and repeated hanging wall K-1 to K-2 units penetrated by the Exeter Deepe 11-22 well (NE SW 22 T1N, R69W). The Deepe well and the nearby Omega Steinbaugh 1 (NW NW 22, T1N, R69W) both show a hanging wall imbricate between the K-5 detachment and the repeat K-1 to K-2 section. In all, five wells have shallow logs showing repeats of units in the K-1 to K-5 interval east of the ramp (Fig 4). Three of these wells (#19-21), including the Deepe and Steinbaugh wells, are shown on cross section B-B' (Plates 1 and 3). East of the leading edge truncation of K-1 to K-5 units (blue dotted line on Fig. 4), all thrusts above the decollement involve units younger than the K-5 horizon (purple squares on Fig. 4).

In addition to section repeated by thrusts, there are examples of section cut out along the decollement and by normal faults that sole into the decollement. Figure 6 shows the thickness of the K-1 to K-2 interval, the section carried immediately above the decollement across the western part of the allochthon. The unit exhibits a regional northwest-trending stratigraphic thick that is interrupted by abrupt thins at and west of the decollement ramp. In these areas the section thins by half from over 200 feet to just over 100 feet (Fig. 6). In most cases, the thinning is

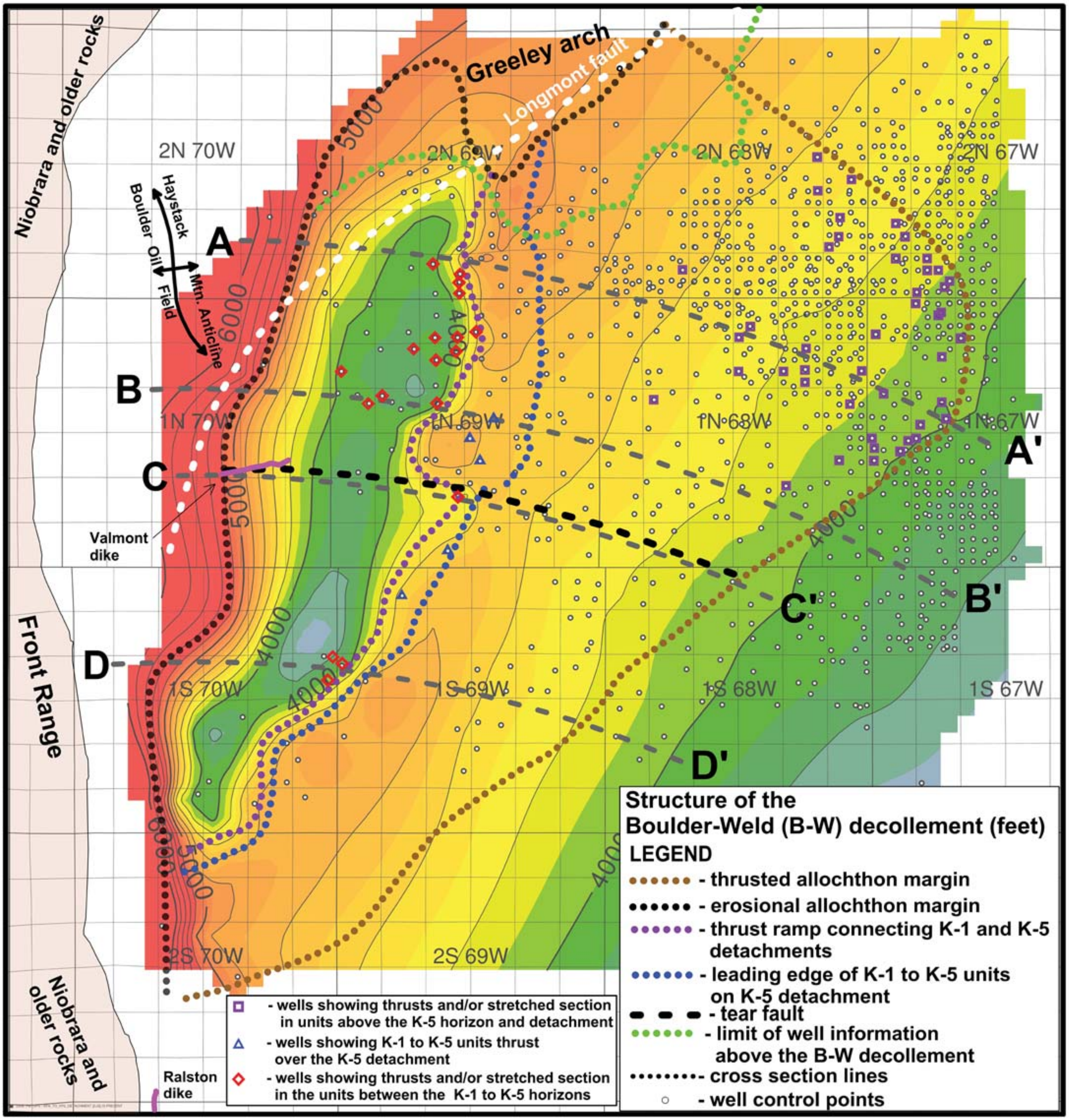

Figure 4. Structure of the Boulder-Weld (B-W) decollement (feet). The decollement dips east off the Front Range and Greely arch, enters a low across the western portion of the Boulder-Weld allochthon (BWA), rises to the east across a thrust ramp, then follows regional dip down to the southeast. The decollement is not cut by the Longmont fault. The western margin of the BWA is erosional, indicating it once extended to the west.

caused by attenuation of the hanging wall at the decollement (blue squares on Fig. 6). In detail, the well logs in this area show the thinning is caused by increasing attenuation of the K-1 to K-2 interval from east to west above the decollement (Fig 7). The attenuation varies along strike, likely reflecting undulations or scalloping in the original trajectory of the decollement. While this attenuation causes a dramatic change in the isopach map, the rate at which beds are cut out is very low indicating the decollement is still almost bedding-parallel across this area. Over a distance of 1.5 miles, 44 feet of section are cut out indicating the decollement cuts across bedding at an angle of approximately 0.3 degrees (see wells between sections 19 and 21 in T1N, R69W). The attenuation either indicates a very low angle normal fault or a thrust cutting gradually down-section in the direction of transport.

Figure 7 also shows the abrupt change in attenuation between wells drilled only a half mile apart in sections 19 and 30 of T1N, R69W. This may reflect lateral offset on the postulated tear fault as discussed below.

There are also examples of normal faults cutting the hanging wall and soling into the decollement. Several of these occur along the decollement ramp and indicate extensional overprint of the earlier thrust. The faults show up as partial attenuation of the units above the decollement ramp (well #8 on section A-A', Plate 1; well #2 on section C-C' and well #4 on section D-D', Plate 2). The only other normal fault seen in this study is the Kolb fault, which lies along the western margin of the BWA as discussed below.

A POSTULATED TEAR FAULT ABOVE THE BWA DECOLLEMENT

The central part of the BWA is cut by a postulated tear fault (Figs. 4, 6 and 7). As noted previously, the tear fault became apparent when an east-west section was drawn that crossed it and showed a confusing pattern of greater translation in the eastern part of the BWA than to the west. The tear fault appears most prominently above a shift in the K-1 to K-5 thrust ramp where it marks a pronounced change in the amount of translation. Figure 4 shows the position of the ramp (purple dots) and leading-edge truncation of K-1 to K-5 units carried up and east of the ramp

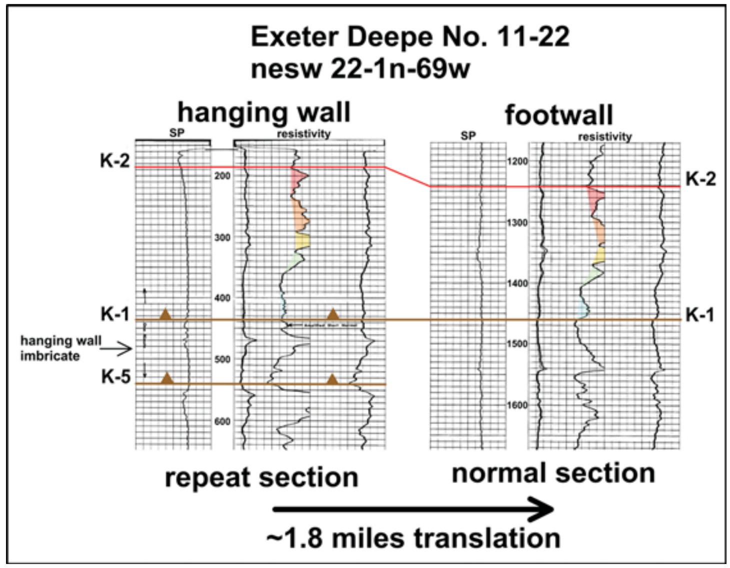

Figure 5. Well log showing repeat of the K-1 to K-2 interval over the K-5 portion of the Boulder-Weld (B-W) decollement. This well shows a repeat of Pierre Shale units in the core of a ramp anticline developed east of the decollement thrust ramp. Wells in this area demonstrate up to two miles of translation of the Boulder-Weld allochthon.

(blue dots). The separation of the two lines provides a measure of translation in the system. North of the tear fault, there are up to two miles of translation, while only three quarters of a mile or less are evident to the south. The tear fault appears to be gently arcuate and is drawn provisionally as a great circle. To the east, it separates northern areas with larger coherent fault blocks bounded by faults with greater throw from the areas to the south showing less throw on thrusts and smaller fault blocks (Spencer, 1986; Roberts et al., 2001). The eastern margin of the BWA does not appear to be offset by the tear fault (Fig. 4), which may reflect poor well control for the margin of the BWA in this area. However, the eastern position of the tear was chosen to coincide with lateral changes in the thrust trends as mapped in detail by Spencer (1986) using coal mine information. Alternatively, the tear fault may not offset the BWA margin and changes in the amount of translation across the tear may be taken up by thrusts interior to the BWA. A tear fault pattern like this appears in the gravity slides surrounding the Bearpaw Uplift of Montana, a possible analog for the BWA as discussed below (Baker and Johnson, 2000; Caldwell, 2008). To the west, the tear fault may be marked between closely spaced wells by an abrupt change in the amount of attenuation seen above the BWA

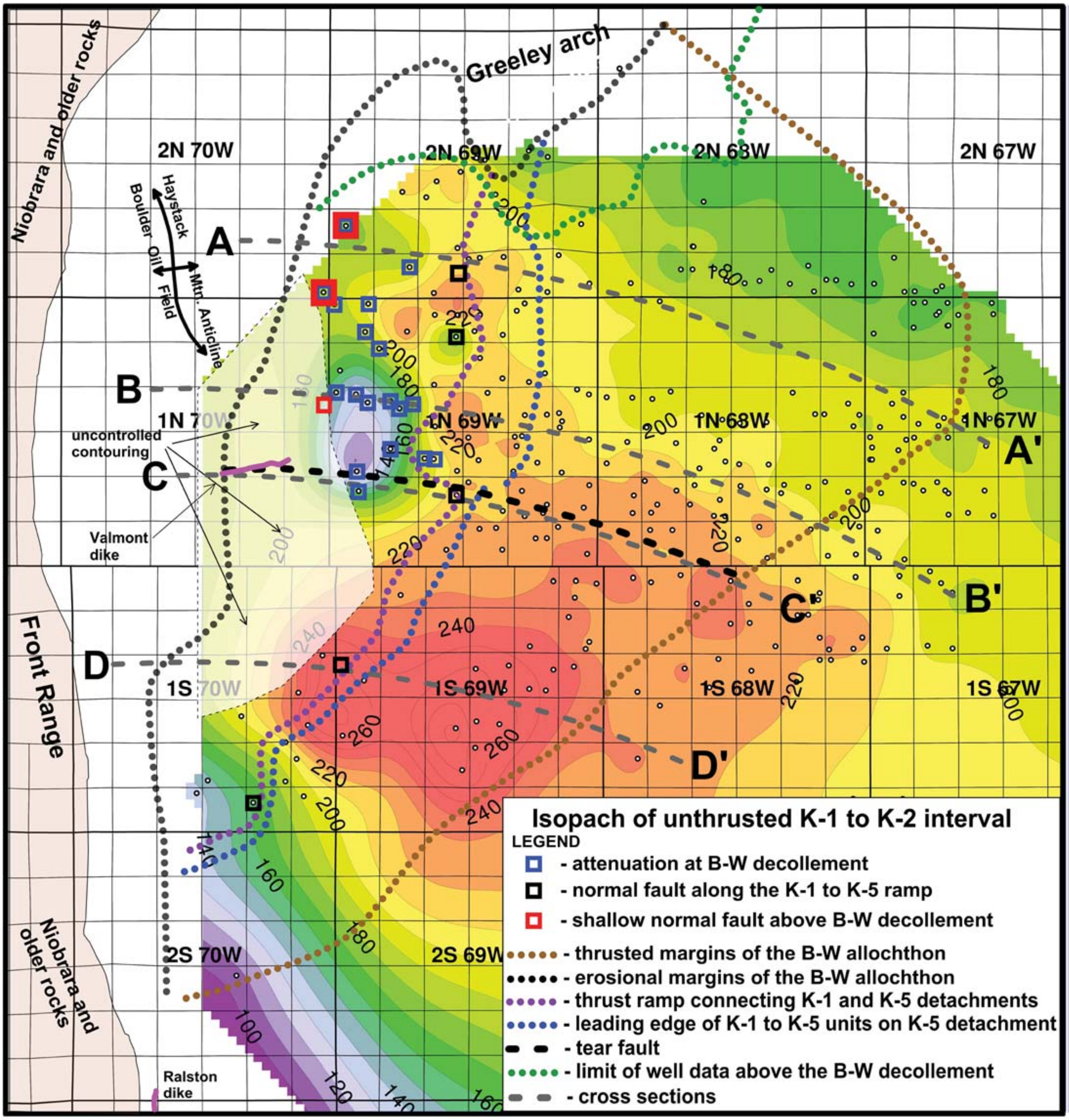

Figure 6. Isopach of the unthrusted K-1 to K-2 interval showing areas with attenuation at the Boulder-Weld (B-W) decollement, normal faults along the K-1 to K-5 ramp and hanging wall normal faults. This map shows attenuation along the western margin of the Boulder-Weld allochthon that could either indicate a very low-angle breakaway normal fault or a thrust cutting gradually down-section in the direction of transport.

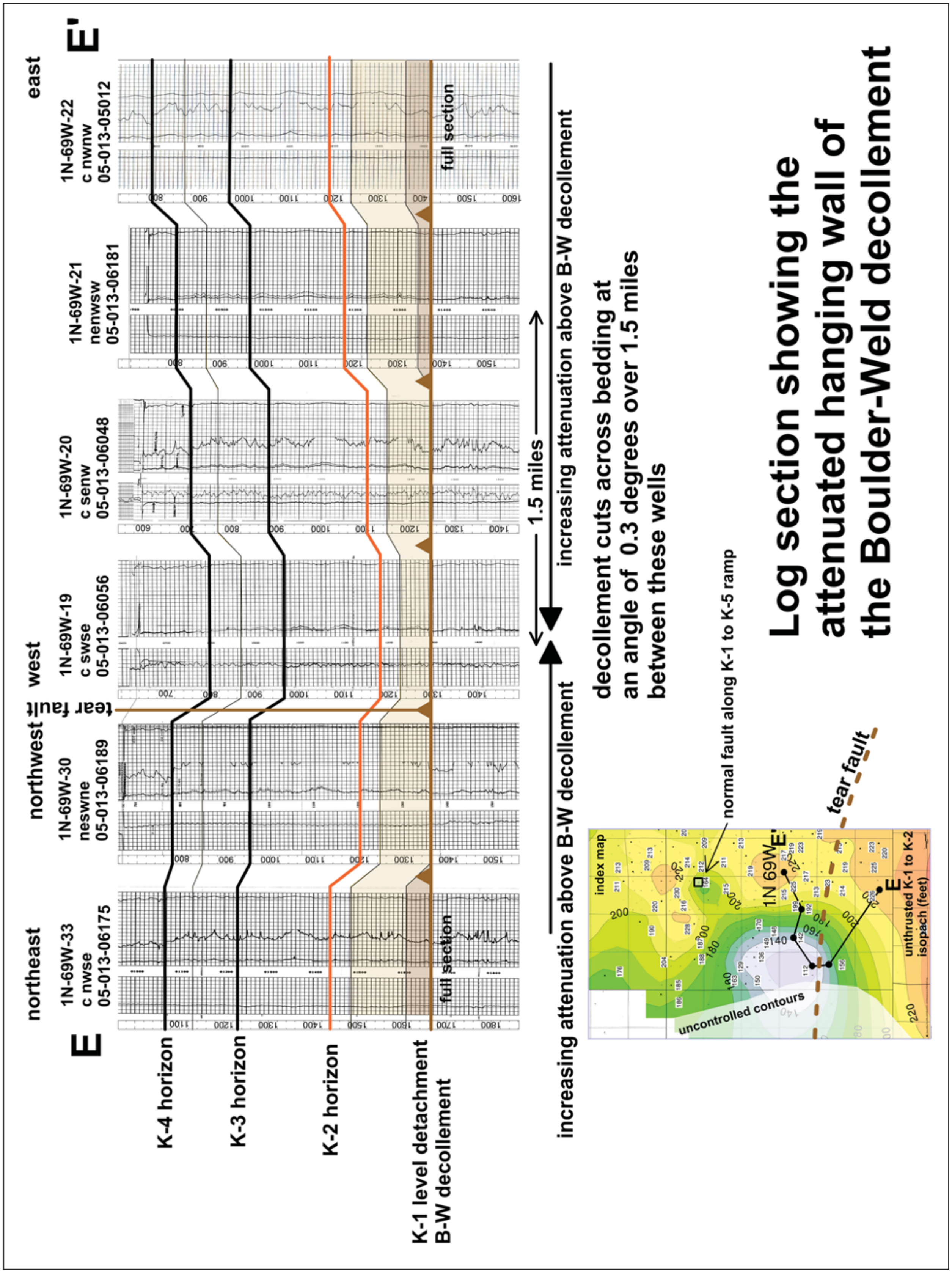

Figure 7. Log section showing the attenuated hanging wall of the Boulder-Weld (B-W) decollement. This section shows the gradual westward attenuation of units above the decollement and the abrupt change in the amount of attenuation across the postulated tear fault.

decollement (wells in 19 and 30 of 1N, 69W on Fig. 7). Once the trace of the postulated tear fault was projected to the western margin of the BWA, it was found to cross the Valmont dike (23, 1N-70W, Fig. 4) with only a twelve-degree difference in their alignments. Its close alignment with the dike may be further evidence for the existence and location of the postulated tear fault.

OUTCROP PATTERNS

Outcrop and near-surface patterns show the gentle east dips on the western flank of the Denver Basin disrupted by faults of the BWA, and further reveal elements of the allochthon (Fig 8.). East of the Haystack Mountain anticline and the Greeley arch, the Fox Hills outcrop belt is interrupted by reappearances of the underlying Pierre Shale. The most prominent of these is a 13-mile long anticline known in the 1930's as the "Louisville structure" when it was tested by Continental Oil's Borra No. 1 well (SW Sec. 5, 1S, 69W) (Barb, 1946). The anticline reflects K-1 to K-5 units breached to the surface where they are carried up the decollement ramp and thrust over a detachment paralleling the K-5 horizon. To the west and east, smaller patches of older rocks surrounded by younger units mark the locations of secondary high blocks carried by imbricates above the decollement.

Figure 8 also shows the traces of thrusts and normal faults based on outcrop patterns, fieldwork conducted for this project, the work of Spencer (1986) and Roberts et al. (2001), the various quadrangle maps referenced earlier, and shallow seismic surveys in the Rocky Flats area (Davis, 1980; Ebasco Team, 1992, 1993a).

FAULTS IN THE HANGING WALL OF THE BWA DECOLLEMENT

One of the principal objectives of this study was to determine the attitudes of faults in the BWA including, where possible, their direction and sense of slip. This involved field checking exposures of faults reported in the literature and finding new exposures. Faults in the White Rocks area are described below and shown in detail on Plate 4 (Sterne and Raynolds, 2019). Details of the fault observations are tabulated on Table 1.

The work started in the western part of the BWA with an examination of the Big fault (NE 18, 1N-69W) at White Rocks. It has been described in the literature as both a reverse fault (Weimer, 1973) and a growth fault with apparent normal offset (Davis and Weimer, 1976). The conflicting descriptions of its geometry offered the possibility it could be part of a breakaway zone for the BWA (Ken Kittleson, pers. comm.), and called for the fault to be reexamined. Access to the restricted White Rocks open space was granted by the City of Boulder Open Space and Mountain Parks Department (OSMP). The White Rocks area offers the best exposures of the Fox Hills Formation in the Denver Basin and an excellent exposure of the Big fault (Weimer, 1973; Trimble, 1975; Weimer and Tillman, 1980). The fault is an east-dipping, west-directed thrust exhibiting well-developed reverse Riedel shears and east-southeast trending slickenlines (Fig. 9). The thrust is penetrated by wells in the SE NE 18, 1N, 69W (Pl. 1 B-B', well # 9) and in the SW 7, 1N, 69W. Possible splays of the fault continue to the north. One splay was mapped by Trimble (1975) along the north line of NW 6, 1N, 69W. We did not find the fault exposed, but beds in its immediate footwall are dragged into an overturned fold indicating west-directed thrust movement. A more easterly splay cuts across 31, 2N, 69W where we found east-dipping slip surfaces (Somerset locale) with well-developed reverse Riedel shears and east-west slickenlines. Just to the east, the splay is penetrated by wells in 32 and 33, 2N, 69W (Pl. 1, A-A', wells #5 and #6) and water wells show Pierre Shale carried close to the surface by the thrusts.

One-half mile east of the Big fault at White Rocks, trenching showed the Ertl fault to be a north- to northwest-dipping thrust, but no fault plane ornamentation was observed (Table 1). Based on changes in outcrop dips (Pl. 4, SW 8, 1N, 69W), the fault continues north and may appear again in 33, 2N, 70W (Pl. 1, A-A', well #6).

The Big and Ertl faults bound an upthrown block or pop-up structure. As shown by a panel of high east dips in outcrop (Pl. 4) and a penetration of its ramp by the well in NW NW 17, 1N, 69W (Pl. 1, B-B', well #10), the Big fault is the master fault with the Ertl fault as its antithetic. Balancing the structural interpretation required recognizing this linkage of the thrusts, with the Ertl fault showing more translation than the Big fault. Such pop-up structures bound by linked antithetic thrusts appear across the BWA. Recognition of this style made it possible to meld the shallow structure in coal mines across the eastern part of the BWA, as mapped by Spencer (1986), with deeper faults encountered in the oil and gas wells.

Three quarters of a mile west of the Big fault, the prominent outcrops of the Fox Hills Formation at White

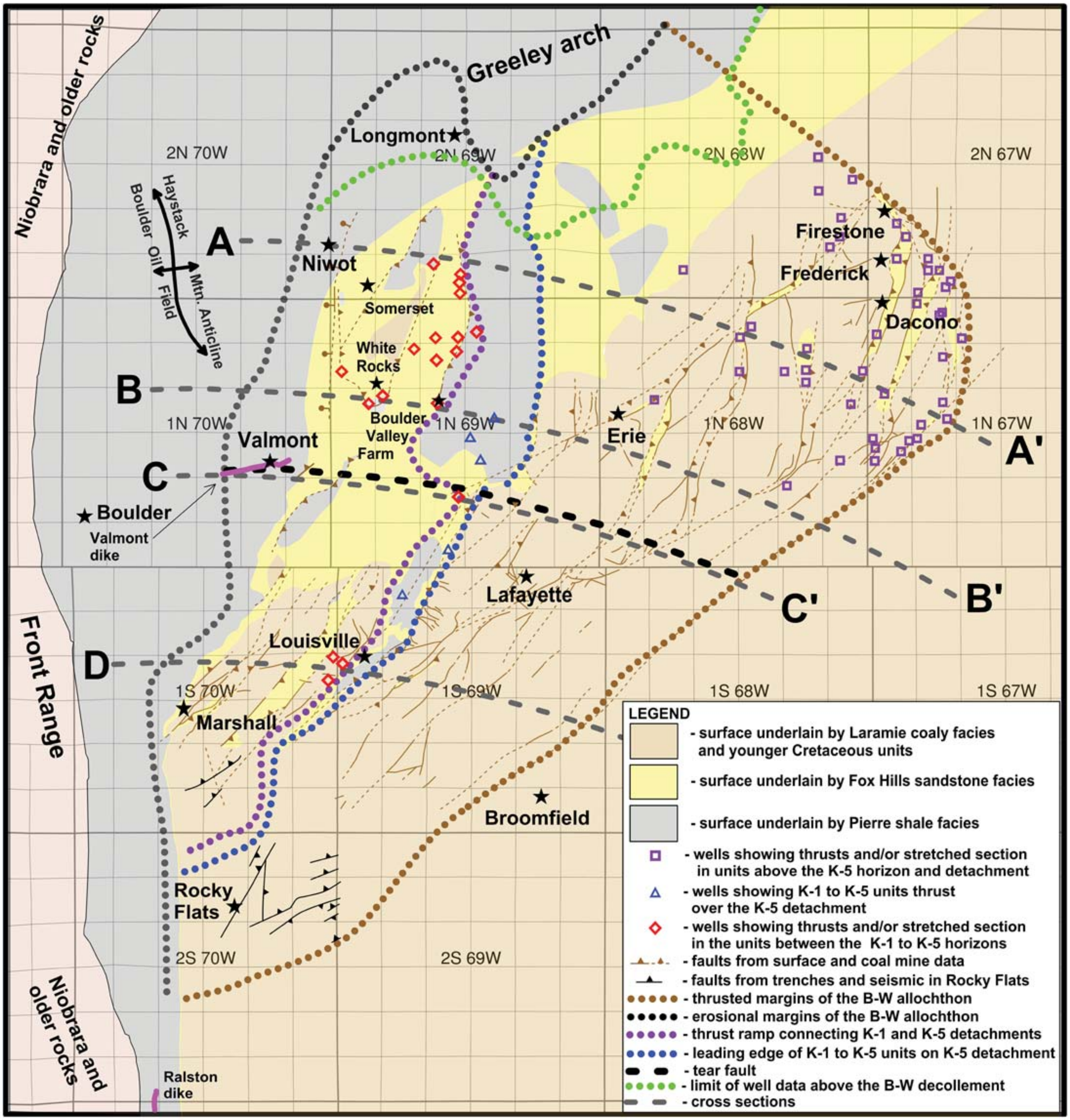

Figure 8. Surface units, fault trends and levels of thrusting across the Boulder-Weld allochthon. This map shows the gentle western flank of the Denver basin interrupted by faults of the Boulder-Weld allochthon. Most prominent is the narrow belt of surface Pierre Shale that marks the trend of the anticline developed east of the decollement ramp.

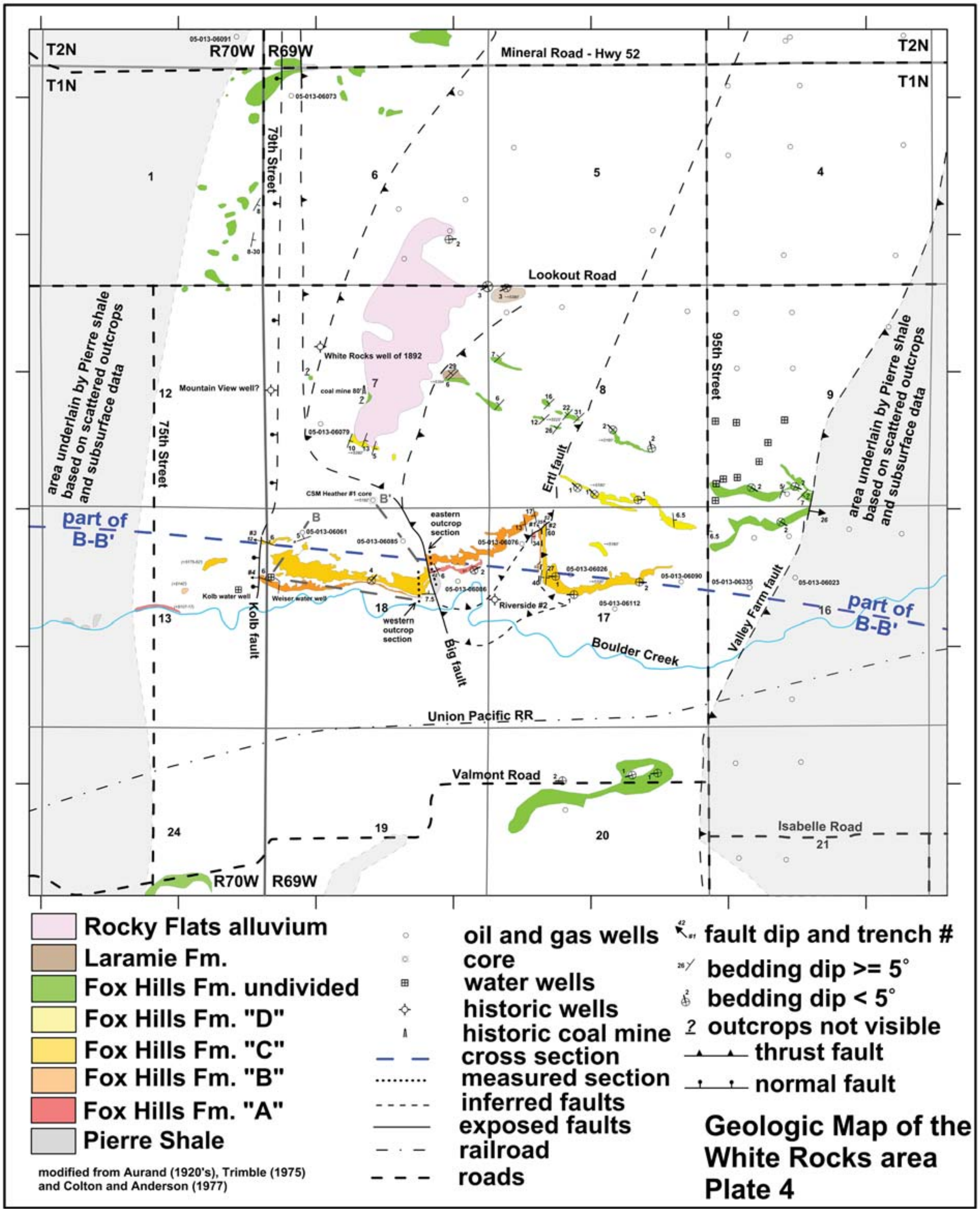

Plate 4. Geology map of the White Rocks area, Boulder County, Colorado.

TABLE 1

A compilation of fault attitudes, slickenline orientations, and Sigma 1 directions reported for the Boulder-Weld allochthon and neighboring Front Range.

Fault name	location	structural domain	slickenline trend-plunge		fault strike-dip RHR			reference
Somerset	SE 31 2N-69W	BWA	093-13		028-14			Sterne and Raynolds (2019)
Big	NE 18-1N-69W	BWA	102-39		345-42			Sterne and Raynolds (2019)
Ertl	NW 17-1N-70W	BWA	NA		295-44			Sterne and Raynolds (2019)
Kolb	NE 13-1N-70W	BWA	NA		355-52			Sterne and Raynolds (2019)
Valley Farm	NW 16-1N-69W	BWA	073-23		028-31			Sterne and Raynolds (2019)
Valley Farm	NW 16-1N-69W	BWA	124-31		028-31			Sterne and Raynolds (2019)
Peerless	SENENE 21-1S-70W	BWA	104-57		045-61			Sterne and Raynolds (2019)
Boulder	SW 36-1N-71W	Front Range	101-34		037-37			Sterne and Raynolds (2019)
Boulder Reservoir	SE-3-1N-70W	Front Range			296-41			Sterne and Raynolds (2019)
Valmont	SW 24-1N-70W	BWA	295-44		057-49			Risk Engineering (1994)
			slickenline trend-plunge 1st_eigenvectors/ 1st_eigenvalues	slickenline number of analyses	fault strike-dip RHR 1st_eigenvectors/ 1st_eigenvalues	faults number of analyses	Sigma 1	
Six Mile fold	SE 25-2N-71W	Front Range	085-16/0.8701	91	NA	NA	088-10	Allen (2010)
Hoosier	24 1S-71W	Front Range	092-39/0.5522	263	305-68/0.4695	263	107-09	Selvig (1994)
Livingston combined	12-13, 2S-71W	Front Range	078-72/0.5874	660	339-21/0.5789	660	075-08	Selvig (1994)
Livingston east-dipping faults		Front Range	076-54/0.7982	404	337-37/0.7964	404		Selvig (1994)
Livingston west-dipping faults		Front Range	253-53/0.7784	257	172-35/0.7756	257		Selvig (1994)
Marshall combined	20-22, 28 1S-70W	BWA	100-10/0.5780	111	330-85/0.6717	202	149-04	Selvig (1994)
Marshall station #1	NESENE 21-1S-70W	BWA	285-01/0.8892	13	005-78/0.6393	28		Selvig (1994)
Marshall station #4	NWNESE 21-1S-70W	BWA	142-44/0.9692	3	255-75/0.7655	28		Selvig (1994)
Marshall station #5	SWNWNW 28-1S-70W	BWA	247-14/0.7964	25	207-68/0.8434	25		Selvig (1994)
Marshall station #6	NWNWNW 28-1S-70W	BWA	106-06/0.5702	8	035-76/0.8139	21		Selvig (1994)
Marshall station #7	SESESE 20-1S-70W	BWA	249-01/0.7253	8	253-29/0.5780	15		Selvig (1994)
Marshall station #11	NWNENE 21-1S-70W	BWA	126-01/0.7085	5	155-77/0.7491	15		Selvig (1994)
Marshall station #13	SENENE 21-1S-70W	BWA	104-38/0.9319	17	048-47/0.9150	17		Selvig (1994)
Marshall station #14	NWNWNW 22-1S-70W	BWA	105-22/0.7821	8	348-69/0.7940	8		Selvig (1994)
Marshall station #16	NWNENW 22-1S-70W	BWA	124-30/NA	9	057-69/0.7750	9		Selvig (1994)

Rocks are terminated by the Kolb fault. Several west-dipping fractures cut the outcrop and the west-dipping fracture face bounding the outcrop was trenched but no fault ornamentation was observed (Table 1). Nonetheless, the Kolb fault appears to be a west-dipping normal fault based on water wells located on either side of the fault (Pl. 1, B-B', wells #4 and #5) indicating the base of the Fox Hills Formation drops down to the west. The Kolb fault continues to the north where it was mapped by Trimble (1975) along the northern bound of NW 6, 1N, 69W. The fault is not exposed, but west-dipping fractures cut the western limits of the Fox Hills Formation east of the fault similar to those seen at White Rocks. Closely-spaced wells drilled on either side of the fault (NW NW 6, 1N, 69W; SE SE 36, 2N, 70W, Pl. 1, A-A', well #4) show the west side is dropped down on a normal fault that cuts out 140 feet of section. One and a half miles farther north, another well (SE NW 30, 2N, 69W) shows 40' of missing section. These relationships show the Kolb fault extends at least 4.5 miles along strike. It does not offset the BWA decollement and there is no data to indicate it is cut by the BWA decollement. Therefore, it is shown here to sole into the BWA decollement. Except for the normal faults seen along the decollement ramp it is the only normal fault encountered across the BWA in this study. There are possible indications of reverse offset associated with the fractures east of the fault at White Rocks (Scott Minor, pers. comm.) suggesting the fault could be an early thrust overprinted by extension. This observation may indicate extensional overprint of Laramide faults similar to that noted by Allen (2010) along the neighboring Front Range. The other possibility is it is part of a breakaway zone developed along the western margin of the BWA.

The Boulder OSMP also allowed access to the Boulder Valley Farm where an exposure of the Valley Farm fault was examined (NE NE NW, 16, 1N, 69W). The fault dips to the east-southeast and is a west-directed thrust that puts Pierre Shale over the Fox Hills Formation (Sterne and Raynolds, 2019). Two sets of lesser-quality slickenlines indicating approximate west-directed slip are evident, and one of the sets shows reverse Riedel shears (Scott Minor, pers. comm.) (Table 1). The fault extends to the northeast parallel to the decollement ramp (Colton and Anderson, 1977) and appears to sole into the top of the decollement ramp as shown in sections A-A' and B-B' on Plate 1.

Field checks of several faults in the Marshall area corroborated the mapping by Spencer (1961), and the east-southeast slickenline orientations measured by Selvig (1994) on the west-directed Peerless thrust (SE SW 15, 1S, 70W) (Table 1).

The exposure of the Valmont Fault in S2 Sec. 24, T1N, R70W as detailed by Risk Engineering (1994) was found to be mostly covered and did not yield any new information (Table 1). Faults shown by Cole and Braddock (2009) cutting the regional layer west of the BWA at Boulder Reservoir were not found, likely due to recent landscaping along the shoreline; however, two east-dipping thrusts are exposed in Pierre Shale outcrop along the shoreline between the dam structures (NW SE 3, T1N, R70W) (Table 1).

The margin of the Valmont Dike (SW SE Sec. 22, T1N, R70W) was examined in the hope of finding slickenlines associated with differential slip along the postulated tear fault that projects across the location of the dike. Horizontal slickenlines were found on the southwestern margin of the dike, but because this part of the dike lies in the footwall of the BWA, the slickenlines likely reflect lateral intrusion of the dike or lateral slip on a fault in the regional layer rather than movement of the postulated hanging wall tear fault.

The area east of the leading edge truncation of the K-1 to K-5 intervals above the K-5 level detachment is where Kittleson (1992, 2009) first described the style of decollement thrusting seen across the BWA. In constructing

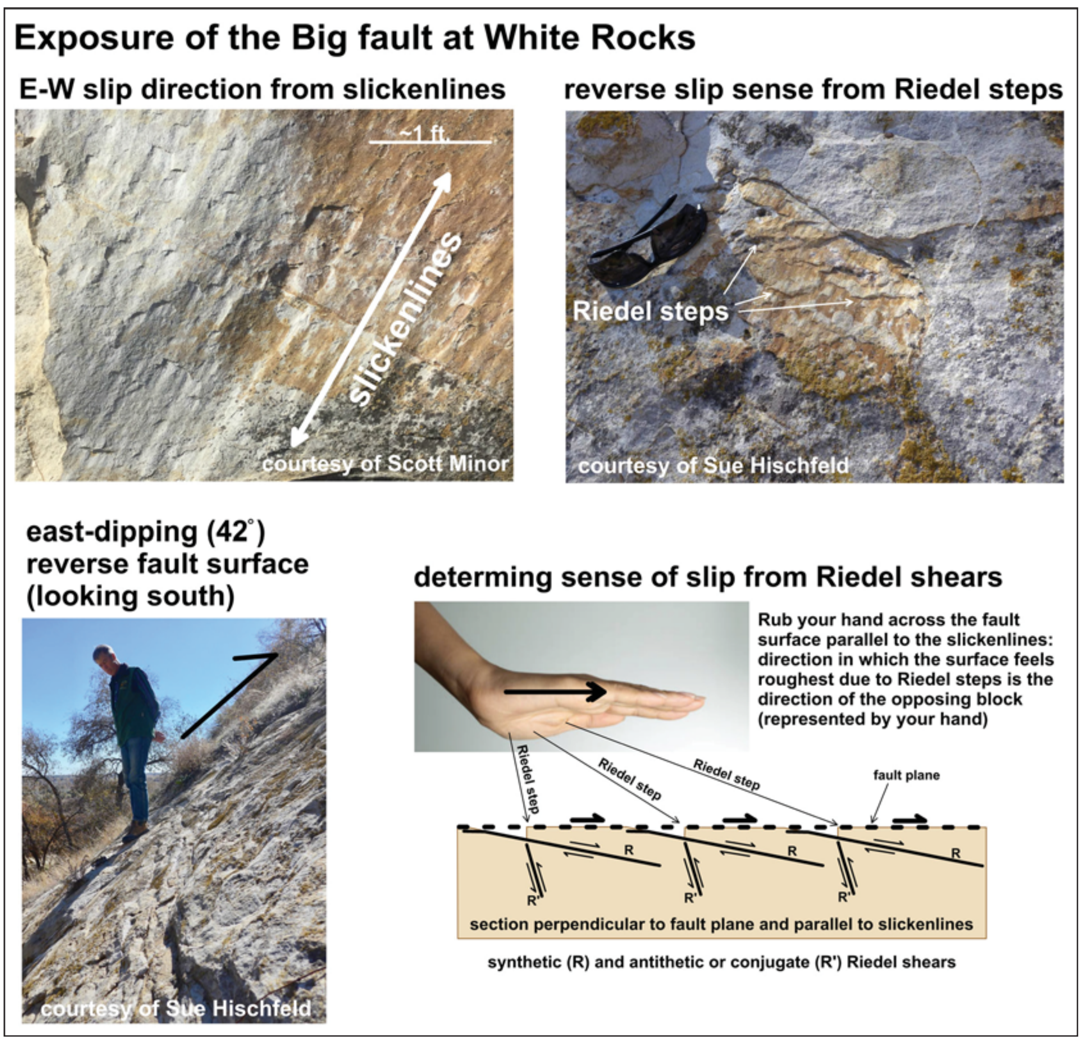

Figure 9. Exposure of the Big fault at White Rocks. The fault plane of the Big fault is beautifully exposed at in the Boulder City White Rocks open space. Reverse Riedel shears and well-developed slickenlines show an east-southeast slip direction, similar to those found across the western portion of the Boulder-Weld allochthon and the neighboring Front Range.

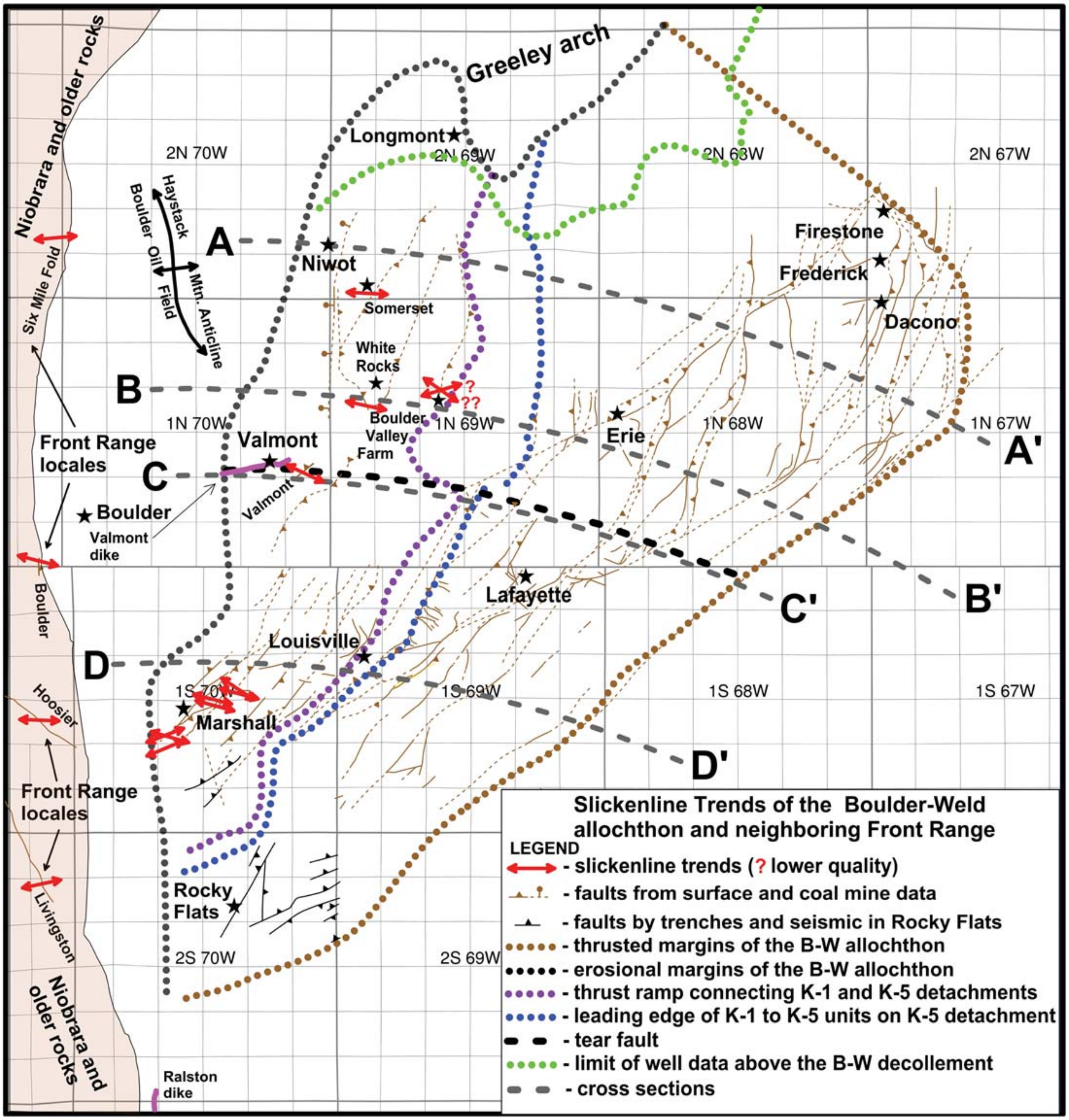

Figure 10. Slickenline trends of the Boulder-Weld allochthon (BWA) and neighboring Front Range. Both the BWA and neighboring Front Range exhibit approximate east-west slickenline trends suggesting but not proving a common genesis for their faults.

cross sections across the eastern area for this study, the basal Laramie Formation C Coal structure map of Spencer (1986) was used to guide the structural interpretation except where available well data contradicted his interpretation. Spencer (1986) showed the faults of the BWA as steep, deep-seated reverse and normal faults. In adapting his information to a style showing lower-angle thrusts as used here, the fault positions marking the known margins of subsurface coal mines were honored as hard data when drawing the cross sections, while the surface locations of the faults were not considered fixed by the subsurface data, and do not appear immediately above the deep fault cuts .

In the absence of shallow oil and gas log data, Spencer's (1986) study of coal mines, coal exploration cores and water wells provides the best means of getting a comprehensive view across this shallower part of the BWA east of the decollement ramp. Another excellent set of data in this area are the four cores cut for the siting of the Weld County Meteorological Observation Facility (Ameudo and Ivey, 1975) (16 1N, 68W, Fig. 1). The report provides detailed dip information and the core holes were logged with gamma ray, resistivity and density tools. Combining these with two deep oil and gas wells (wells #30-35 on B-B', Plate 1), a picture emerges of a thrust structure bounded on both sides by linked, antithetic faults; a style reminiscent of the thrust structure seen in older units to the west in White Rocks and best described as a pop-up structure. Numerous examples of this kind of structure are shown in the cross sections (Plates 1-3) across the eastern part of the BWA.

Surface traces of faults mapped across the Erie quadrangle (Colton and Anderson, 1977) were checked in the hopes of finding fault exposures across the eastern part of the BWA. This several-day effort was not successful due to a predominance of shaley facies giving poor outcrops and extensive development that has destroyed many of the outcrops.

SLIP DIRECTIONS BASED ON SLICKENLINE TRENDS

Figure 10 and Table 1 show slickenline orientations for the western part of the BWA and the neighboring Front Range. The data are a compilation of measurements made during this study and those reported in the literature (Selvig, 1994; Risk Engineering, 1994; Allen, 2010). Slickenline orientations from Risk Engineering (1994) and this study are single measurements or averages of a low number of measurements. Risk Engineering's (1994) description of the Valmont fault provides the fault strike and dip (237-49 FHR), and slickenline orientation and rake (295-40). Their slickenline orientation of 295° is honored in Table 1 and Fig. 10, however, the reported rake suggests a slickenline orientation of 266°, which is more in line with other slickenline orientations along the western margin of the BWA. The slickenline orientations from Selvig (1994) and Allen (2010) are based on first eigenvectors and reflect multiple measurements. The slickenline orientations vary from east-northeast to east-southeast, indicating an overall east-west slip direction in both areas.

Currently, slickenline data are only available along the western part of the BWA. Field checks along mapped surface faults in the Erie area have so far yielded no new slickenline data due to extensive Quaternary cover or recent development. The arcuate trend of the tear fault suggests slip directions in the eastern part of the BWA will arc to the southeast in close agreement with the slip direction implied by the orientation of sections drawn in this part of the system by Kittleson (1992, 2009). The cross sections prepared for this study parallel the trend of the tear fault and provide provisional predictions of local slip directions.

SUMMARY BLOCK DIAGRAM OF THE BWA

Figure 11 summarizes the structural elements of the BWA. The allochthon moved up to two miles east on its basal decollement above a gently southeast-dipping regional layer. From its western outcrop trace, the decollement cuts down-section to the east along an attenuation fault cutting at an extremely low angle to bedding (0.3 degrees) before merging into a bedding-parallel detachment at the K-1 horizon. Across this part of the allochthon, the attenuated hanging wall rides on the K-1 level detachment and secondary thrusts and a normal fault cutting the hanging wall sole into the K-1 level detachment. To the east, the BWA travels approximately 900 feet up-section on a thrust ramp connecting the K-1 level detachment to a shallower, bedding-parallel detachment at the K-5 horizon (equal to the Kp2 horizon of Kittleson (1992, 2009)). Immediately east of the ramp, units between the K-1 and K-5 horizons are thrust over the K-5 level detachment. A west-directed thrust detached at the K-5 horizon is thought to branch off the decollement at the leading-edge truncation of the K-1 to K-5 units and takes up about half or more of the eastward translation. East of this truncation and to the eastern limit the allochthon, the decollement rides parallel to the

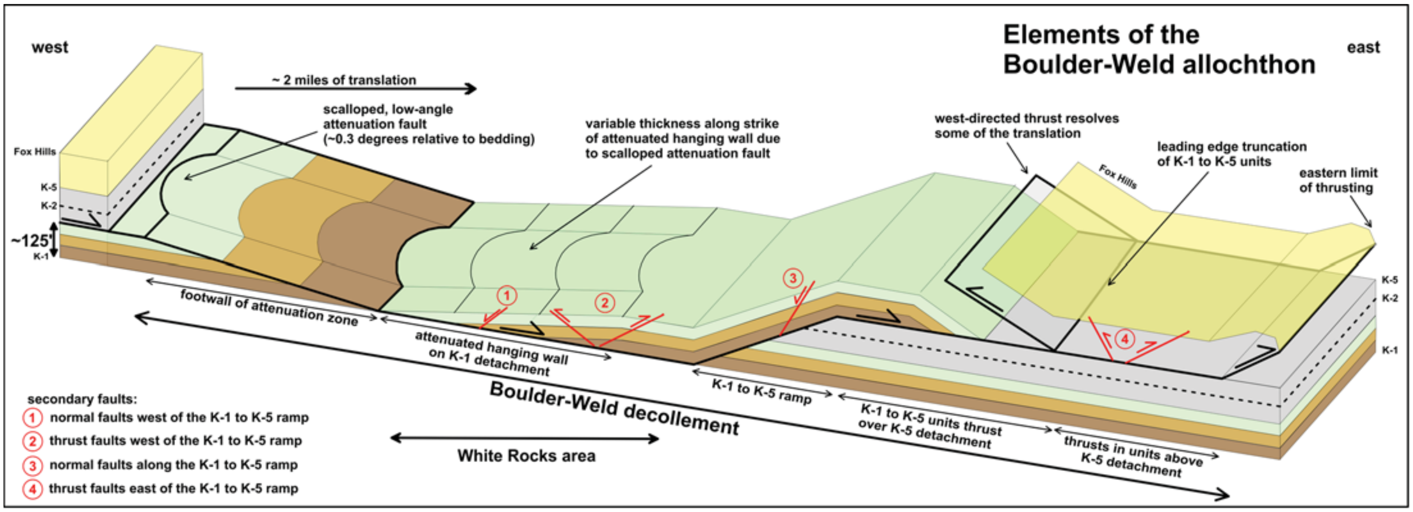

Figure 11. Block diagram showing elements of the Boulder-Weld allochthon.

K-5 horizon, and secondary thrusts cutting hanging wall K-5 and younger units sole into the K-5 level detachment. The block diagram best typifies the northern part of the BWA with the near face representing a postulated arcuate tear fault cutting from west to east across the central part of the system. Geometries south of the tear fault are similar. Translation of the BWA decreases from two miles north of the tear fault to three quarters of a mile or less south of the tear fault.

TRANSLATION AMOUNTS WITHIN THE BWA

Plate 3 posts measures of translation at different points in the system. There are two ways to calculate translation for the system depending on the assumed genetic model and how normal fault offsets are treated. In a gravity slide, both normal faults and thrusts contribute to the translation of the system, while in a thrust system only thrusts add to translation of the system and normal faults may obscure the amount translation on earlier thrusts. These differences only come into play for areas at and west of the ramp where normal faults occur.

In the case of a gravity slide: 1) secondary structures west of the ramp show between 0.2 and 0.3 miles of translation, 2) at the leading edge cutoff of the K-1 to K-5 units east of the ramp the system shows between 0.3 and 1.8 miles of translation, while 3) east of the truncation between 0.3 and 0.8 miles of translation are evident.

Assuming a thrust origin: 1) thrusts west of the ramp show between 0.05 and 0.3 miles of translation, 2) at the leading edge cutoff of the K-1 to K-5 units east of the ramp the system shows between 0.3 and 1.8 miles of translation, while 3) east of the truncation between 0.3 and 0.8 miles of translation are evident.

North of the tear fault the system loses about half of its translation on a west-directed back thrust detached at the K-5 horizon. Using triangle zone terminology (Jones, 1996), this can be thought of as a roof thrust accommodating some of the eastward translation on the decollement or floor thrust. This feature could be drawn as an east-directed thrust; however, the west-directed interpretation meshes better with the patterns shown by Spencer (1986) along the northern leading-edge truncation. South of the tear, the amount of translation seen at the leading-edge truncation east of the ramp equals the translation seen on thrusts farther to the east, suggesting the back thrust is not present south of the tear. No wells have been found showing faults above the decollement across the eastern area south of the tear. The thrust structures shown on section C-C' are controlled by Spencer's (1986) mapping of the Laramie Formation C Coal. Section D-D' lies south of Spencer's map and thrust trends were taken from the mapping of Roberts et al. (2001) with the cumulative throw on the thrusts east of the leading-edge truncation drawn to match the translation at the ramp. Future work on this line should incorporate water well data to better constrain the interpretation.

TIMING OF THE BWA

Control for the timing of Laramide thrusting in the Front Range bracket their movement to between 67 Ma and 55 Ma (Kluth and Nelson, 1988; Raynolds, 1997; Caine et al., 2006; Dechesne et al., 2011; Siddoway et al., 2013; Barkmann et al., 2016). Paleomagnetic studies of Laramide structures along the mountain front west of the BWA show: 1) sills near Boulder dated to 64.6+-2.4 Ma were injected during thrusting, and 2) sills at Ralston (four miles south of Rocky Flats) dated to 61.9+-2.5 Ma were injected prior to thrusting (Hoblitt and Larson, 1975) .

Thrusts of the BWA offset units as young as the Arapahoe Conglomerate in the Rocky Flats area (Ebasco Team, 1992, 1993a), so its development occurred after 67 Ma. Claims of syndepositional thinning across high blocks of the BWA offered as evidence for growth faulting during deposition of the Laramie Formation by Rahmanian (1975) were disproven by Spencer's (1986) detailed analysis of coal mine data. Furthermore, Trudgill (2015) provides no evidence of syndepositional faulting in support of his model showing inversion of early growth faults by thrusts in the Marshall area. If the Valmont dike played a role in creating the postulated tear fault, the BWA formed either at or later than the emplacement of the dike which dates to 64.9+-2.6 Ma (Larson and Drexler, 1994) or 64.0+-5.0 Ma (Musselman, 1987). These dates indicate the BWA could have formed during or after the Laramide orogeny.

DISCUSSION

By recognizing the style of decollement thrusting that characterizes the BWA, Kittleson (1992, 2009), as corroborated by Selvig (1994), made the conceptual breakthrough that is the basis for this study. However, my analysis shows a somewhat different structural picture of the BWA than presented by Kittleson (1992, 2009), and indicates a different transport direction than calculated by Selvig (1994). These differences do not disprove the gravity slide models of these authors, but do leave open the possibility the BWA formed as a Laramide thrust sheet.

Kittleson's (1992, 2009) model for the BWA called for a gravity slide moving one-half mile to the southeast from a breakaway headwall at the Longmont fault. The movement was thought to occur above a detachment paralleling a single stratigraphic horizon in the upper part of the Pierre Shale (His Kp2 horizon equal to the K-5 horizon). No faulting was recognized below this detachment. Hanging wall structures were thought to include normal faults associated with a breakaway zone to the west and east-vergent reverse faults or toe thrusts to the east.

In contrast, the current study shows:

1) The Longmont fault folds, but does not cut the BWA decollement. Therefore, the Longmont fault does not form the breakaway headwall for the BWA. The decollement simply rises to the west and daylights at the surface, indicating the BWA once extended farther to the west and its current western limit is erosional.

2) The BWA decollement ramps ~900' up-section to the east from a near bedding-parallel detachment low in the upper transition member of the Pierre Shale (K-1 level), to a bedding-parallel detachment near the base of the Fox Hills Formation (K-5 level).

3) Units above the deeper, K-1 detachment are carried up the decollement ramp and over the shallower K-5 detachment. The leading-edge truncation of these older units shows up to two miles of translation of the BWA.

4) Attenuation of section along the decollement and the presence of the Kolb normal fault in its hanging wall may be remnants of a breakaway zone along the western margin of the BWA. Alternatively, the attenuation zone may reflect a thrust cutting slightly down section in the direction of transport. The hanging wall normal faults may represent extensional overprinting of older thrusts.

5) Pop-up structures bound by east- and west-directed antithetic thrust faults are a common style across the BWA.

Slickenline data across the western margin of the BWA and the neighboring Front Range show a shared, approximate east-west slip direction (Table 1, Fig. 10), which differs from the conclusion reached by Selvig (1994) in his comparison of the two areas.. As shown by Erslev and Larson (2006), average slickenline and ideal Sigma1 trends for structures across the Laramide foreland are directly correlative, indicating average slip direction and average compression direction will be the same. This relationship held true for all of the slickenline localities reported by Selvig (1994) and Allen (2010) except for the Marshall area in the southwestern part of the BWA. There, Selvig (1994) reported a slickenline first eigenvector oriented to 100 degrees and an average Sigma1 orientation of 149 degrees (Table 1). The 49 degree difference between these values could indicate the kind of clockwise stress rotations associated with northeast-trending Laramide faults in the northeastern Front

Range (Larson, 2009). Or, the stress inversion may have a difficult time deriving Sigma1 in the complex fault arrays at Marshall. Selvig (1994) used the calculated Sigma1 vector to interpret the Marshall thrusts as south-southeast directed toe thrusts in a gravity-driven system; however, the near east-west slickenline trends support rather than preclude a linkage to Laramide thrusting.

SUPPORT FOR THE GRAVITY SLIDE MODEL

The gravity slide genesis for the BWA is best supported by the attenuation zone developed along the western side of the BWA. In this model, the attenuation zone would represent the remnant of a very low-angle, east-directed normal fault forming the principal failure surface of a breakaway zone. The hanging wall ramp of the normal fault would have been carried east onto the bedding-parallel detachment at the K-1 horizon where it is now preserved in the subsurface. The Kolb fault could be a preserved example of higher-angle normal faults developed above and soling into the master breakaway fault along the western side of the system.

Possible gravity slide analogs for the BWA include such systems as the deep-water thrust belts found on passive margins (Rowen et al., 2004), and megaslides such as the Heart Mountain in Wyoming (Malone et al., 2014) and the Marysvale in Utah (Hacker et al., 2014; Biek et al., 2020). However, the best analog in terms of age, tectonic setting and structural style is the gravity slide system surrounding the Laramide Bearpaw Uplift of Montana as described by Reeves (1946), Baker and Johnson (2000) and Caldwell (2008) and summarized from their work below. The structures involve Upper Cretaceous rocks detached at two horizons in marine shales of the Marias River Formation. The detachments carry shoreline sandstones of the Eagle Formation and marine shales of the overlying Claggett Formation radially off the domal uplift. Hanging wall structures include normal faults in breakaway zones at the crest of the uplift, toe thrusts along its flanks, and tear faults internal to the system. Many of the thrust structures are pop-ups bound by antithetic faults. Seismicity during Eocene igneous activity and loading of the Cretaceous rocks by Eocene volcanics are thought to have triggered the down-flank movement of the slides.

Emplacement of the Bearpaw, Heart Mountain and Marysvale gravity slides all involved coeval igneous and volcanic activity (Reeves, 1946; Malone et al., 2014; Hacker et al., 2014; Biek et al., 2020). Volcanic loading primed the slides, and coeval intrusions and related seismicity are cited as triggers for their catastrophic collapse.

Unlike the examples above, the BWA is not part of a large volcanic field. However, sills, dikes and small plugs scattered along the Front Range between Ralston (located 4 miles south of Rocky Flats) and the Six Mile fold attest to igneous activity in proximity to the BWA during the Paleocene (Kellogg et al., 2008; Cole and Braddock, 2009). In addition, Paleocene volcanic fields, associated with the Colorado Mineral Belt, that once covered much of the Front Range adjacent to the BWA (Raynolds, 1997), could have set the conditions for a large gravity slide similar to the megaslides noted above.

A more speculative trigger mechanism evoking seismicity related to seal rupture by overpressured hydrocarbons could explain why the BWA developed above the southwest corner of the giant Wattenberg oil and gas field (Fig. 1). This part of the field is the locus of the "Wattenberg hot spot", an area named for its elevated thermal maturity, high bottom-hole temperatures, reservoir overpressures, and high gas-oil-ratios of produced hydrocarbons (Higley et al., 2007). Hydrocarbons generated in the Mowry and Dakota have migrated several thousand feet up-section through much of the Pierre Shale and now produce from the Hygiene and Terry sandstones in the shallow Spindle Field (Clayton and Swetland, 1980), which straddles the eastern margin of the BWA. Resistivity logs "light up" across the Pierre Shale indicating the presence of a hydrocarbon chimney in this part of the field (Steve Cumella, pers. comm.). Clearly, oil and gas have migrated vertically through a thick layer of what should be sealing shales. Hydrocarbon migration through shales is likely caused by natural hydraulic fracturing driven by overpressures (Engelder and Lacazette, 1990). The most likely place in the field for a catastrophic seal breach would have been the Wattenberg hot spot, which lies immediately northeast of the BWA. It is difficult to prove a rupture of this type created seismicity to trigger the BWA as a gravity slide. However, there is a growing body of literature that attributes earthquakes and aftershocks up to magnitude 6 to seal rupture by high-pressure carbon dioxide (e.g. Miller et al., 2004). In a case involving hydrocarbons, Lacazette (1991) studied porosity development due to natural hydraulic fracturing by high-pressure, methane-saturated brines in the Ordovician Bald Eagle Formation of central Pennsylvania. He cites an example of a gas reservoir that vented during an ancient seal rupture. Fluids drove explosively to the surface, thereby opening breccia channels that facilitated later meteoric water invasion to depths of 9 kilometers. It is likely that a catastrophic event such as this could have triggered the BWA as a gravity slide either by decreasing friction along its decollement or by spawning seismicity. Timing of the seal breach is likely post-Laramide. Higley and Cox (2007) modeled the burial history of the Cretaceous "D" and Muddy ("J") sandstones using a well located near the Wattenberg hot spot. They found onset of generation during the Laramide. However, peak gas generation, which would have been associated with the seal breach, occurred later during upper Eocene to Miocene time (40-20 Ma). Maturation within the hot spot may have begun earlier, but if the BWA was triggered by a catastrophic seal breach it likely formed after the Laramide. One interesting aspect of the catastrophic seal breach model is that it is the only mechanism discussed here that explains why the BWA is a unique feature along the Front range, and why it lies on top of the Wattenberg Field.

SUPPORT FOR THE LARAMIDE THRUST SHEET MODEL

East-west slip directions seen on faults across the western part of the BWA and the neighboring Front Range show they may share a common Laramide thrust origin. Their other common trait is the stratigraphic level at which they detach. The BWA is detached near the top of the Pierre Shale, which is the detachment level for the main strand of the Golden fault system and other Laramide thrusts south along the range front (Sterne, 2006).

However, the presence of an attenuation zone, which may represent the breakaway fault for a gravity slide, poses the biggest problem for the Laramide thrust model. Thrusts typically parallel bedding or cut up-section in the direction of transport. But there are exceptions, especially in areas with preexisting structure. While there are no prominent structures east of the mountain front that would have been cut by the decollement, Cole and Braddock (2009) mapped several northeast-trending faults cutting the regional footwall west of the BWA at Boulder Reservoir, and my fieldwork showed two east-dipping thrust faults in the same area (Table 1). Wells are rare in this position along the mountain front; however, a well in the SE NE 3, T3N, R70W is cut by two minor thrusts in the lower part of the Pierre Shale. Any of these could have presented a step in the regional layer that caused the decollement to cut down-section locally in the direction of transport. Recall, this divergence is small, with the decollement cutting at an angle of 0.3 degrees relative to bedding, so the decollement rides almost parallel to bedding across the attenuated area. Another explanation for the attenuation along the decollement could relate to extensional overprint on a preexisting thrust, similar to that noted by Allen (2010) in the Laramide systems along the mountain front. In this case, a west-directed thrust branching off the decollement may have reversed out with its hanging wall ramp translated east onto the decollement.

There are several trajectories the BWA decollement may have followed to link westward with the Laramide thrust systems. As noted earlier, deep well and seismic control make it clear the BWA does not simply root westward into the subsurface along the flank of the Front Range, rather its decollement breaches to outcrop and is eroded away to the west. This means any link to thrusting along the mountain front is now gone. There could be east-directed faults along the east flank of the mountain front that cut up-section and link to the east-directed BWA above the current ground level. However, a deliberate search of the few wells in this position along the mountain front and of seismic lines extending east of the mountain front reveal no thrusts that could account for the 0.7 to 2 miles of translation exhibited by the BWA. The remaining possibility is the decollement rises to the west and links as an east-directed roof thrust resolving translation in the system of west-directed Laramide thrusts present along the flank and into the interior of the range (Fig. 12).

Roof thrusts of triangle zones and wedge thrust systems typically rise in the direction of transport, but there are exceptions (Jones, 1996). Medwedeff (1992) presented cross sections controlled by closely spaced wells from the Wheeler Ridge anticline of California. The sections show a wedge thrust system where the roof thrust climbs over the axis of the underlying ramp anticline then dips in the direction of its transport down the back flank of the anticline. This is the same general configuration of the thrusts shown on Figure 12 where the roof thrust climbs over the axes of multiple west-directed ramp anticlines then dips east in the direction of its transport down the back flank of the thrust stack. The deformed section with its restored geology above the current topographic surface is based

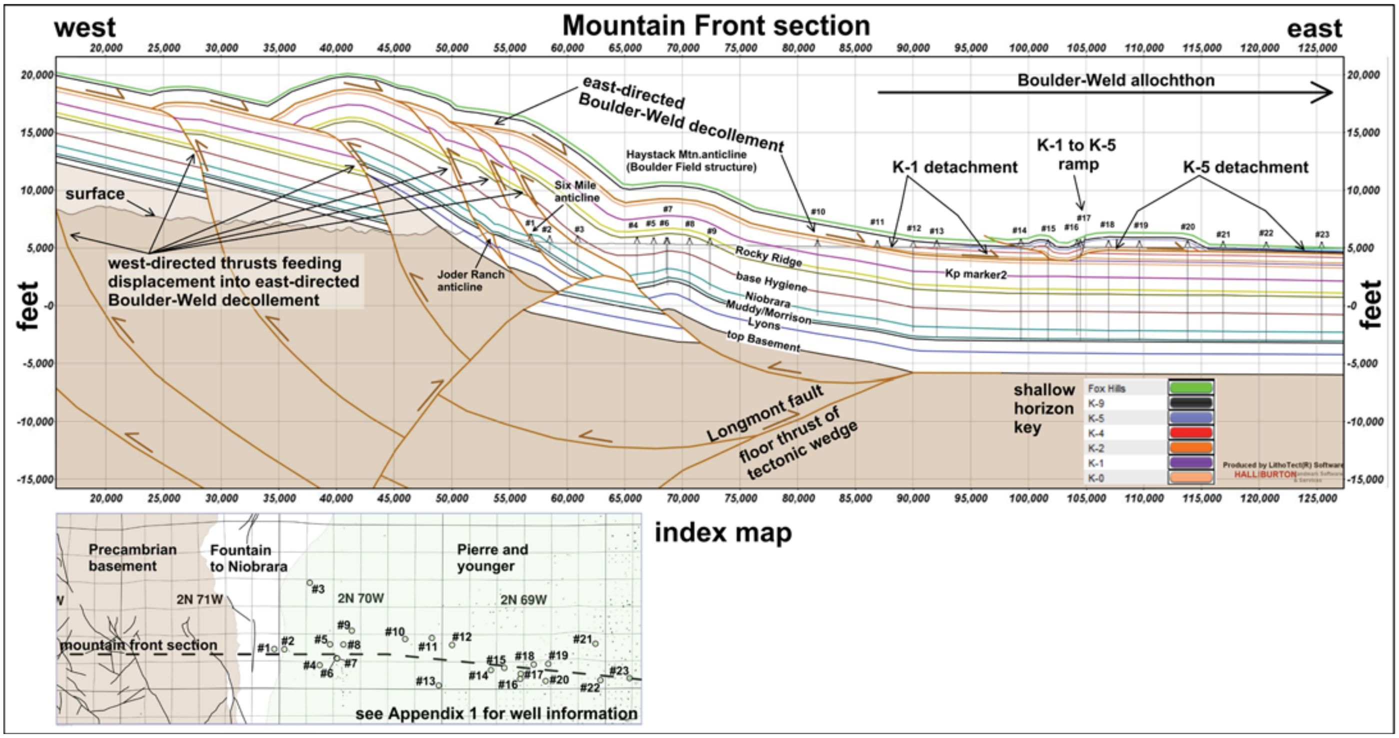

Figure 12. Cross section modeling the Boulder-Weld allochthon as an east-directed passive roof thrust resolving translation on Laramide thrusts of the neighboring Front Range. This cross section illustrates the hinterland-directed thrusts that dominate the northern Front Range, a thrust vergence opposite that seen along most thrust fronts. The west-directed thrusts may have set up an atypical roof thrust that is directed toward the foreland and that dips in the direction of its transport.

on a palinspastic restoration. While throw on each of the west-directed basement thrusts is not known, the Rogers thrust, where seen west of Rocky Flats, shows up to 5000 feet of west-directed throw (Wells, 1967; Sterne, 2019) based on offset of the Crescent Mountain syncline axis. The Front Range is not the usual thrust front where faults verge to the foreland. As shown on Figure 12, all of the thrusts along the mountain front except for one are west-directed. West-directed thrusts dominate the Front Range from the Rocky Flats area and to the north (Erslev, 1993; Selvig, 1994; Larson, 2009). Such atypical conditions could lead to the development of an atypical foreland-directed, foreland-dipping roof thrust.

CONCLUSIONS

This effort has redefined key elements of the Boulder-Weld allochthon (BWA), in particular across the western part of the system. The BWA moved up to two miles east off the flank of the neighboring Front Range and Greeley arch, then appears to have rotated to the southeast following the fall line of the Denver Basin. The allochthon currently covers 216 mi^2 (559 km^2), but its western margin is erosional indicating it is the remnant of a once larger system. Along its western margin the BWA decollement is detached near the base of the upper transition member of the Pierre Shale. To the east, the decollement ramps up-section some 900’ to a higher detachment near the base of the Fox Hills Formation.

Both the decollement and faults in its hanging wall show a mix of characteristics indicating contraction and extension. These geometries can be interpreted as related to gravity sliding or Laramide thrusting. For the gravity slide interpretation, attenuation present along the western margin of the decollement, and hanging wall normal faults located along the decollement ramp and to the west can be interpreted as elements of a breakaway zone. The decollement thrust ramp, its associated ramp anticline, and the numerous thrust bounded pop-up structures in its hanging wall can be interpreted as gravity-driven toe thrusts.

Alternatively, the mix of contractional and extensional features can be interpreted as Laramide thrusts overprinted by later extension such as noted in the neighboring Front Range (Allen, 2010). The decollement ramp, its associated ramp anticline, and numerous hanging wall thrust structures can interpreted as Laramide thrust geometries. Attenuation along the western margin of the decollement can be attributed to a thrust cutting slightly down-section in the direction of transport. Normal faults in the hanging wall of the decollement can be explained by extensional overprint of preexisting thrusts.

Analogs exist to support either of these models. The gravity-driven breakaway normal faults and toe thrusts systems surrounding the Bearpaw Uplift of Montana offer one analog for the gravity slide model (Reeves, 1946; Baker and Johnson, 2000; Caldwell, 2008). A more speculative trigger for the gravity slide may have been seismicity spawned by a catastrophic seal rupture in the underlying Wattenberg oil and gas field. Wedge thrust and triangle zone systems showing roof thrusts dipping in the direction of transport (e.g., Medwedeff, 1992) offer the best thrust analog for the BWA decollement. The decollement can be interpreted as an east-dipping, east-directed roof thrust resolving throw on the west-directed basement thrusts that dominate the northern part of the Front Range (Fig. 12).

Both the BWA decollement and Laramide thrusts of the neighboring Front Range utilize detachments near the top of the Pierre Shale (Sterne 2006, 2019). In addition, both systems exhibit similar approximate east-west slickenline trends indicating a common slip direction. These similarities suggest a possible link between the BWA and Laramide thrusting, but do not preclude its origin as a gravity slide

If the BWA is related to thrusting, it would have formed during the Laramide. Timing for its possible origin as a gravity slide is less certain. If it was triggered by volcanic loading or seismicity related to igneous activity as evoked for the analog Bearpaw system, it could have formed during nearby Paleocene volcanism that was concomitant with Laramide thrusting (Hoblitt and Larson, 1975). Or, it may have been spawned by more distant post-Laramide volcanism known to have occurred elsewhere in the Front Range (Raynolds, 1997). If the BWA formed as a gravity slide triggered by seismicity related to a catastrophic seal breach in the underlying Wattenberg oil and gas field, it would have mostly likely taken place in post-Laramide time as hydrocarbon generation peaked (Higley and Cox, 2007).

This study provides a different and more comprehensive picture of the structure of the BWA. What it does not answer is its origin. Both gravity slide and Laramide thrust origins for the Boulder-Weld allochthon are viable and admissible, meaning they honor the observed data and can be supported by analogs. It remains for future studies to test these hypotheses and to determine if they are true.

ACKNOWLEDGEMENTS

The following people and institutions are thanked for making this study possible. I am indebted to Ken Kittleson for his recognition of decollement thrusting in the eastern parts of the BWA and our subsequent discussions regarding the nature and location of its postulated breakaway zone. These led me to look at the Big fault in the White Rocks area to which both reverse and normal offset had been attributed. Rick Groshong joined these discussions in 2019 in an effort to balance thrust structures in the eastern part of the BWA. Entry to the restricted parts of the White Rocks open space was authorized by Lynn Riedel of the City of Boulder Open Space and Mountain Parks Department and facilitated by volunteer geologist Sue Hirschfeld. Bob Raynolds joined me in a "quick" study of the stratigraphy and structure of White Rocks, which soon ballooned to encompass all of the BWA in an effort to frame the novel structural features we were seeing in the surface and subsurface data. Fault trenching in the open space was done under the watchful eye of Christian Driver, archeologist for the City of Boulder. Scott Minor, U.S.G.S. structural geologist emeritus, put his keen eye to the structural fabrics across the area. Colorado School of Mines provided access to their Heather #1 core of the Fox Hills Formation. The U.S. Geological Research Facility allowed us to examine their D612 core across the Laramie and Fox Hills formations, and the upper part of the Pierre Shale. CTL Thompson, Inc. graciously provided a copy of the Ameudo and Ivey (1975) engineering report describing shallow cores at the Weld County Meteorological Observing Facility. Steve Cumella is thanked for his sage technical assistance. Connie Knight kindly loaned copies of the shallow seismic and trenching reports for Rocky Flats. The Denver Earth Resources Library provided access to several key well logs not available through the COGCC. Maria Henry generously provided the Petra software that facilitated analysis of the oil and gas wells. Halliburton provided the LithoTect software used to construct the cross sections. Finally, David Malone of Illinois State University and John Singleton of Colorado State University are thanked for providing very helpful reviews of the manuscript.

REFERENCES

Allen, C.L., 2010, Timing and genesis of fractures in the Niobrara Formation, northeastern Front Range and the Denver Basin, Colorado: Master's thesis, Colorado State University, Fort Collins, Colorado, 200 p.

Ameudo C.L. and Ivey, J.B., 1975, Engineering geology investigations, proposed Joint Meteorological Observing Facility tall tower, Weld County, Colorado: Robert W. Thompson, Inc., Denver, Colorado, 36 p.

Baker, D.W. and Johnson, E.H., 2000, Tectonic framework and gas-filled structures of the Bearpaw Mountains, North-Central Montana: Montana Geological Society 50th Anniversary Symposium Montana/Alberta Thrust Belt and Adjacent Foreland, v. 1, p. 1-26.

Barb, C.F., 1946, Selected well logs of Colorado: Colorado School of Mines Quarterly, v. 41, n. 1, 435 pp.

Barkmann, P.E., Sterne, E.J., Dechesne, M., and Houck, K.J., 2016, South Park, Colorado: The interplay of tectonics and sedimentation creates one of Colorado's crown jewels: *in* Keller, S.M., and Morgan, M.L., eds., Unfolding the Geology of the West: Geological Society of America Field Guide 44, p. 151-190, DOI: https://doi.org/10.1130/2016.0044(07).

Bedwell, J. L., 1974, Textural parameters of clastic rocks from borehole measurements and their application in determining depositional environments: Ph.D. dissertation, Colorado School of Mines, Golden, Colorado, 215 p.

Biek, R.F., Rowley, P.D., and Hacker, D.B., 2020, Utah's ancient mega-landslides: Utah Geological Survey, Survey Notes, v. 52, no. 2, p 1-3.

Caine, J.S., Nelson, E.P., Beach, S.T., and Layer, P.W., 2006, Structural fabrics, mineralization, and Laramide kinematics of the Idaho Springs-Ralston shear zone, Colorado Mineral Belt and central Front Range uplift: The Mountain Geologist, v. 43, no. 1, p. 1-24.

Caldwell, M. 2008, Exploration for gravity fault controlled structural traps, north-central Montana: Back to Exploration - CSPG CSEG CWLS Convention, p. 937-940.

Clayton, J.L. and Swetland, P.J., 1980, Petroleum generation and migration in the Denver Basin: The American Association of Petroleum Geologists Bulletin, v. 64, no. 10, p. 1613-1633, DOI: https://doi.org/10.1306/2f9196d4-16ce-11d7-8645000102c1865d.

Cole, J.C. and Braddock, W.A., 2009, Geologic map of the Estes Park 30' by 60' quadrangle, north-central Colorado: U.S. Geological Survey Scientific Investigations Map 3039 and pamphlet, 56 p, DOI: https://doi.org/10.3133/sim3039.

Colton, R.B. and Anderson, L.R., 1977, Preliminary geologic map of the Erie quadrangle, Boulder, Weld and Adams counties, Colorado: U.S. Geological Survey Misc. Field Studies, Map MF-882, DOI: https://doi.org/10.3133/mf882.

Colton, R.B., and Lowrie, R.L., 1973, Map showing mined areas of the Bolder-Weld coalfield, Colorado: U.S. Geological Survey Misc. Field Studies, Map MF-513, DOI: https://doi.org/10.3133/mf513.

Dechesne, M., Raynolds, R.G., Barkmann, P.E., and Johnson, K.R., 2011, Notes on the Denver Basin geologic maps: bedrock geology, structure, and isopach maps of the Upper Cretaceous to Paleogene strata between Greeley and Colorado Springs: Colorado, Denver Museum of Nature and Science and the Colorado Geological Survey, 35 p.

Davis, T.L., 1980, Rocky Flats reflection seismic report, Final Environmental Impact Statement to ERDA 1545-D, Rocky Flats Plant Site Golden, Jefferson County, Colorado: U.S. Department of Energy EIS-0064, p. C-2-1 - C-2-22.

Davis, T.L. and Weimer, R.J., 1976, Late Cretaceous growth faulting, Denver Basin, Colorado: Colorado School of Mines Professional Contributions, no. 8, p. 280-300.

Ebasco Team, 1992, Task 2, Shallow high-resolution seismic reflection program Indiana Street and west spray field: Final Report, Phase II Geologic Characterization Data Acquisition: U.S. Department of Energy SW-A-000407 1992, 120 p.

Ebasco Team, 1993a, Task 2, Additional shallow high-resolution seismic reflection profiling on Indiana Street: Final Report, Phase II Geologic Characterization Data Acquisition: U.S. Department of Energy SW-A-001982 1993, 128 p.

Ebasco Team, 1993b, Task 2, Deep seismic data acquisition from Coal Creek canyon to Great Western Reservoir: Final Report, Phase II Geologic Characterization Data Acquisition: U.S. Department of Energy SW-A 000592 1993, 244 p.

Emmons, S.F., W. Cross, and G.H. Eldridge, 1896, Denver Basin in Colorado: U.S. Geological Survey Monograph 27, 150 p, DOI: https://doi.org/10.5962/bhl.title.45516.

Engelder, T. and Lacazette, A., 1990, Natural hydraulic fracturing: *in* Barton, N., and Stephansson, O., eds., Rock Joints: A.A. Balkema, Rotterdam, p. 35-44.

Erslev, E.A., 1993, Thrusts, back thrusts and detachment of Rocky Mountain fore land arches: *in* C.J. Schmidt, R.B. Chase, and E.A. Erslev, eds., Laramide Basement Deformation in the Rocky Mountain Foreland of the United States: Geological Society of America Special Paper 280, p.339-358, DOI: https://doi.org/10.1130/spe280-p339.

Erslev, E.A. and Larson, S.M., 2006, Testing hypotheses for the Colorado Front Range arch, using minor faults: The Mountain Geologist, v. 43, no. 1, p. 45-64.

Erslev, E.A., and Selvig, B, 1997, Thrusts, back thrusts and triangle zones: Laramide deformation in the northeastern margin of the Colorado Front Range: *in* D.W. Bolyard and S.A. Sonnenberg, eds., Geologic History of the Colorado Front Range: RMAG 1997 RMS-AAPG Field Trip #7, p. 65-76.

Fenneman, N.M., 1905, Geology of the Boulder District, Colorado: U.S. Geological Survey Bulletin 265, 101 p, DOI: https://doi.org/10.3133/b265.

Hacker, D.B., Biek, R.F., and Rowley, P.D., 2014, Catastrophic emplacement of the gigantic Markagunt gravity slide, southwest, Utah (USA): Implications for hazards associated with sector collapse of volcanic fields: The Geologic Society of America Geology, v. 42, no. 11, p. 943-946, DOI: https://doi.org/10.1130/g35896.1.

Haun, J.D., 1968, Structural geology of the Denver Basin – regional setting of the Denver earthquakes: Colorado School of Mines Quarterly, v. 63, no. 1, p. 101-112.

Higley, D.K. and Cox, D.O., 2007, Oil and gas exploration and development along the Front Range in the Denver Basin of Colorado, Nebraska, and Wyoming, *in* Higley, D.K., Petroleum Systems and Assessment of Undiscovered Oil and Gas in the Denver Basin Province, Colorado, Kansas, Nebraska, South Dakota, and Wyoming – USGS Province 39: U.S. Geological Survey Digital Data Series DDS-69-P, ch. 2, 41 p, DOI: https://doi.org/10.3133/ds69p.

Hoblitt, R., and Larson, E., 1975, Paleomagnetic and geochronologic data bearing on the structural evolution of the northeastern margin of the Front Range, Colorado: Geological Society of America Bulletin, v. 86, p. 237-242, DOI: https://doi.org/10.1130/0016-7606(1975)86%3C237:pagdbo%3E2.0.co;2.

Jones, P.B., 1996, Triangle zone geometry, terminology and kinematics: *in* P.A. Mackay, J.L. Varsek, T.E. Kubli, R.G. Dechesne, A.C. Newson, and J.P. Reid, eds., Triangle Zones and Tectonic Wedges: Bulletin of Canadian Petroleum Geology, v. 44, no. 2, p. 139-152.

Keller, S.M. and Morgan, M.L., 2018, Geologic map of the Frederick quadrangle, Weld and Broomfield counties, Colorado: Colorado Geological Survey Open File Report 18-01.

Kellogg, K.S., Shroba, R.R., Bryant, B. and Premo, W.R., 2008, Geologic map of the Denver West 30' by 60' quadrangle, north-central, Colorado: U.S. Geological Survey Scientific Investigations Map 3000 and pamphlet, 48 p, DOI: https://doi.org/10.3133/sim3000.

Kiteley, L.W., 1978, Stratigraphic sections of Cretaceous rocks of the northern Denver Basin, northeastern Colorado and southeastern Wyoming: U.S. Geological Survey Oil and Gas Investigations Chart OC-78, DOI: https://doi.org/10.3133/oc78.

Kittleson, K., 1992, Decollement faulting in the northwest portion of the Denver Basin: The Mountain Geologist, Rocky Mountain Association of Geologists, v. 29, no. 2, p. 65-70.

Kittleson, K., 2009, The origin of the Boulder-Weld fault zone, east of Boulder, Colorado: The Mountain Geologist, Rocky Mountain Association of Geologists, v. 46, no. 1, p. 37-49.

Kluth, C.F. and Nelson, S.N., 1988, Age of the Dawson arkose, southwestern Air Force Academy, Colorado, and implications for the uplift history of the Front Range: The Mountain Geologist, v. 25, no. 1, p. 29-35.

Lacazette, A.J., Jr., 1991, Natural hydraulic fracturing in the Bald Eagle sandstone in central Pennsylvania and the Ithaca siltstone at Watkins Glen, New York: Ph.D. dissertation, The Pennsylvania State University, State College, Pennsylvania, 226 pp.

Larson, E.E. and Drexler, J.W., 1988, Early Laramide mafic to intermediate volcanism, Front range, Colorado: Colorado School of Mines Quarterly, v. 83, no. 2, p. 41-52.

Larson, S.M., 2009, Laramide transpression and oblique thrusting in the northeastern Front Range, Colorado: 3D kinematics of the Livermore Embayment: Master's thesis: Colorado State University, Fort Collins, Colorado, 210 p.; DOI: http://hdl.handle.net/10217/21587.

Malone, D.H., Craddock, J.P., Anders, M.H., and Wulff, A., 2014, Constraints on emplacement age of the Heart Mountain slide, northwestern Wyoming: The Journal of Geology, v. 122, p. 671-686, DOI: https://doi.org/10.1086/678279.

Medwedeff, D.A., 1992, Geometry and kinematics of an active, laterally propagating wedge thrust, Wheeler Ridge, California, *in* Mira, S., and Fisher, G.W., eds., Structural Geology and Fold Belts: The Johns Hopkins University Press, p. 3-28.

Miller, S.A., Collettini, C., Chiaraluce, L., Cocco, M., Barchi, M, and Kaus, B.J.P., 2004, Aftershocks driven by high-pressure CO2 source at depth: Nature 2251, p. 1-4, DOI: http://doi:10.1038/nature02251.

Musselman, T.E., 1987, A modified crustal source for the Colorado mineral belt; implications for REE buffering in CO^2-rich fluids: Master's thesis, Colorado School of Mines, Golden, Colorado, 127 p.

Rahmanian, V.D., 1975, Deltaic sedimentation and structure of the Fox Hills and Laramie formations, Upper Cretaceous, southwest of Boulder, Colorado: Master's thesis, Colorado School of Mines, Golden, Colorado, 83 p.

Raynolds, R.G., 1997, Synorogenic and post-orogenic strata in the Central Front Range, in Bolyard, D.W. , and Sonnenberg, S.A., eds., Geologic History of the Colorado Front Range: Rocky Mountain Association of Geologists 1996 RMS-AAPG Field Trip #7, p. 43-49.

Reeves, F., 1946, Origin and mechanics of the thrust faults adjacent to the Bearpaw Mountains, Montana: Geological Society of America Bulletin v. 57, p. 1033-1048, DOI: https://doi.org/10.1130/0016-7606(1946)57[1033:oamott]2.0.co;2.

Risk Engineering, Inc., 1994, Seismic hazards for Rocky Flats Plant: U.S. Department of Energy Final Report 9217-COO-204, Appendix A, p. 1-57.

Roberts, S.B., Hynes, J.L., and Woodward, C.L., 2001, Maps showing the extent of mining, locations of mine shafts, adits, air shafts, and bedrock faults, and thickness of overburden above abandoned coal mines in the Boulder-Weld coal field, Boulder, Weld and Adams counties, Colorado: U.S. Geological Survey Geologic Investigations Series I-2735, DOI: https://doi.org/10.3133/i2735.

Rowan, M.G., Peel, F.J., and Vendeville, B.C., 2004, Gravity-driven fold belts on passive margins: *in* McClay, K.R., ed., Thrust Tectonics and Hydrocarbon Systems: American Association of Petroleum Geologists Memoir 82, p. 157-182, DOI: https://doi.org/10.1306/m82813c9.

Scott, G. R., and Cobban, W.A., 1965, Geologic and biostratigraphic map of the Pierre Shale between Jarre Creek and Loveland, Colorado: U.S. Geological Survey Misc. Geological Investigations Series Map I-439, DOI: https://doi.org/10.3133/i439.

Selvig, B. W., 1994, Kinematics and structural models of faulting adjacent to the Rocky Flats Plant, central Colorado: Master's thesis, Colorado State University, Fort Collins, Colorado, 132 p.

Spencer, F.D., 1961, Bedrock geology of the Louisville Quadrangle: U.S. Geological Survey Quadrangle Map GQ-151, DOI: https://doi.org/10.3133/gq151.

Siddoway, C.S., Myrow P., and Fitz Díaz, E., 2013, Strata, structures and enduring enigmas: A 125th Anniversary appraisal of Colorado Springs geology, *in* Abbott, L. and Hancock, G.S., eds., Classic Concepts and New Directions: Exploring 125 Years of GSA Discoveries in the Rocky Mountain Region: Geological Society of America Field Guides, v. 33, ch. 13, p. 331-356, DOI: https://doi.org/10.1130/2013.0033(13).

Spencer, F.D., 1986, Coal geology and coal, oil, and gas resources of the Erie and Frederick Quadrangles, Boulder and Weld counties: Colorado: U.S. Geological Survey Bulletin 1619, 50 p, DOI: https://doi.org/10.3133/b1619.

Sterne, E.J., 2006, Stacked, "evolved" triangle zones along the southeastern flank of the Colorado Front Range: The Mountain Geologist, v. 43, no. 1, p. 65-92.

Sterne, E.J., 2019, Palinspastic restoration of the eastern flank of the Colorado Front Range at Coal Creek, constrained by outcrop geology, wells and a pre-stack depth migration of the Rocky Flats deep seismic line, reveals a system of stacked triangle zones: American Association of Petroleum Geologists Datapages, Search and Discovery Article no. 90357, Rocky Mountain Section Meeting, Cheyenne, Wyoming.

Sterne, E.J. and Raynolds, R.G., 2019, Year-end report for 2019 on the geology of the White Rocks Open Space, Boulder County, Colorado: City of Boulder Open Space and Mountain Parks Department, 25 p.

Trimbel, D.E., 1975, Geologic map of the Niwot Quadrangle, Boulder County Colorado: U.S. Geological Survey Map GQ-1229, DOI: https://doi.org/10.3133/gq1229.

Trudgill, B., 2015, Unraveling the geometry and origin of a northeast-southwest striking linked array at Marshall Mesa, western Denver Basin: a (possible) solution through integrated digital mapping: American Association of Petroleum Geologists Datapages, Search and Discovery Article no.10755, Annual Convention and Exhibition, Denver, Colorado.

Weimer, R.J., 1973, A guide to uppermost Cretaceous stratigraphy, central Front Range, Colorado: Deltaic sedimentation, growth faulting and early Laramide crustal movement: The Mountain Geologist, Rocky Mountain Association of Geologists, v. 9, no. 2-3, p. 241-267.

Weimer, R.J., 1996, Guide to the Petroleum Geology of the Laramide Orogeny, Denver Basin and Front Range, Colorado: Colorado Geological Survey Bulletin no. 51, p. 1-127.

Weimer, R.J., and Davis, T.L., 1977, Stratigraphic and seismic evidence for Late Cretaceous growth faulting, Denver Basin, Colorado, *in* Payton, C.E., ed., Seismic Stratigraphy: Applications to Hydrocarbon Exploration: American Association of Petroleum Geologists Memoir 26, p. 277-299.

Weimer, R. J. and Tillman, R.W., 1980, Tectonic influence on deltaic shoreline facies, Fox Hills sandstone, west-central Denver Basin: Society for Sedimentary Geology, SEPM Field Trip Guidebook 2, Colorado School of Mines Professional Contributions, no. 10, 131 p.

Wells, J.D., 1967, Geology of the Eldorado Springs Quadrangle, Boulder and Jefferson counties, Colorado: U.S. Geological Survey Bull. 1221-D, 85 p, DOI: https://doi.org/10.3133/b1221d.

Wrucke, C.T. and Wilson, R.F., 1967, Geologic map of the Boulder Quadrangle, Boulder County, Colorado: U.S. Geological Survey Open File Report 67-281, DOI: https://doi.org/10.3133/ofr67281.

APPENDIX 1.

Wells included in cross sections A-A', B-B', C-C', and D-D'.

p5 Appendix 1 Sterne BWA.xlsx

Please go to file attachments within Acrobat to access the Excel document.

Attachments in Acrobat Reader are accessible by going to View >> Show/Hide >> Navigation Panes >> Attachments.

THE AUTHOR

Edward J. (Ned) Sterne

Ned Sterne received a B.A. in geology from Harvard University in 1979 having finished an undergraduate honors thesis on the Indus-Tsangpo Suture Zone of Ladakh, northern India. He completed an M.A. in geology in 1981 at Dartmouth College after studying ammonium illites associated with exhalative ore deposits in the Delong Mountains of northern Alaska. Following a stint in Rocky Mountain and international petroleum exploration for Amoco from 1981 to 1992, he was an independent play generator and consultant, except for the period of 2004 to 2009 when he worked for Petro-Hunt doing Rocky Mountain exploration. Between 2009 and 2015 he explored as an independent in the Denver Basin and consulted on a variety of domestic and international exploration projects, including regional seismic investigations in the offshore of East Africa and, across the East Russian Arctic Shelf. Since retiring in 2015, he has been studying the geology of Colorado. Ongoing projects include: 1) the palinspastic restoration of a transect following Interstate 70 across Colorado, 2) a structure map on the Rocky Mountain erosion surface across Colorado and parts of neighboring states, 3) a study of domes in the Rocky Mountain piedmont that have controlled river courses, and 4) continued studies of stacked triangle zones along the eastern flank of the Front Range. He gives lectures and field trips and has recently received from the Rocky Mountain Association of Geologists the 2017 Best Speaker Award for a talk describing his collaborative work on the Interstate 70 cross section and the 2018 Distinguished Public Service to Earth Science Award for his efforts to communicate advances in our understanding of geology. His extracurricular activities include long walkabouts, sculpting, and amusing his wife Rosanne, three daughters, two son-in-laws, and one grandson.